UNIVERSIDADE DE LISBOA
FACULDADE DE CIÊNCIAS
DEPARTAMENTO DE BIOLOGIA VEGETAL

Identification and study of lipid metabolism genes by qPCR in Rubisco mutants of *Chlamydomonas reinhardtii*

Miguel Camões Fragoso Gaspar

Mestrado em Biologia Molecular e Genética

Dissertação orientada por:

Prof. Doutora Maria da Glória Esquível
Prof. Doutora Ana Rita Matos

2017

Master's thesis in Molecular Biology and Genetics, Faculdade de Ciências da Universidade de Lisboa, held at Biosystems and Integrative Sciences Institute (BioISI) and Instituto Superior de Agronomia (ISA), under the supervision of Doutora Maria da Glória Esquível and Doutora Ana Rita Matos.

Most of the results described in this thesis were presented at one international scientific meeting:

Gaspar, M, Esquível MG, Matos AR. *Phenotypic characterization of Chlamydomonas reinhardtii mutants that perform a deficient CO_2 assimilation*. 3rd General COST meeting workshop 2017, ITQB NOVA.

I. Agradecimentos

Um grande obrigado a ambas as orientadoras pelo tempo, paciência e dedicação demonstrados ao longo deste ano. Foram uma inspiração e uma força que me permitiram conhecer um pouco da vida académica e ficar a saber mais sobre o que é investigação científica.

Ao meu pai e à minha mãe, pelo tempo e energia e toda a fé que depositaram em mim não só para o mestrado mas na vida. Pela disponibilidade em ouvir os meus desabafos sobre o tema e pela tranquilidade que têm e me ensinaram a ter ao longo destes 23 anos.

À minha avó Zulima e tia Paula, pela preocupação pelo bem-estar das algas e do meu trabalho. Ao Rui Pedro, que mesmo estando longe faz por estar perto. À Alicia, que apareceu em Abril e tornou a família Gaspar mais sorridente. Que um dia consigas tudo aquilo que queiras! O teu sorriso trouxe felicidade do Luxemburgo à Nova Zelândia.

À Dona Manuela, pela ajuda no laboratório e pelo bom ambiente criado. Sem a sua ajuda não teria sido a mesma experiência. Aprendi muito consigo. Nunca perca essa força de vontade.

À Daniela e ao Eduardo, os meus parceiros de tese. Obrigado por tudo. Sem vocês aquele laboratório não tinha aquele ambiente tranquilo mas divertido, de trabalhos diversos mas com intercomunicação. Tornaram a FCUL num lugar de trabalho incrível!

Aos Professores Jorge e Andreia, pela orientação na parte estatística e pela disponibilidade que mostraram ao longo destes meses.

Ao Bernardo, Ana, Rui, Gonçalo, Clemente, João, Bárbara, Filipa, Marco e Jesús, pelos bons momentos no laboratório. Tornaram o processo mais fácil e calmo. Trabalhar rodeado de energia positiva torna tudo mais simples.

À Carina, Marisa e Bárbara, obrigado pelas conversas sobre tudo e sobre nada. Sem vocês o mestrado não tinha sido o mesmo. Obrigado por ouvirem, pelos bons momentos e pela partilha de opiniões.

Ao Iúri, Ana, Marisa, Cláudia e Paulo pelo vosso apoio ao longo da tese. Obrigado por me ouvirem e estarem presentes quando mais importa.

Finalmente, um obrigado ao tio Alexandre e à avó Guida. Não estão cá mas continuam presentes na nossa mente. Obrigado pelas lições de vida.

Um especial obrigado à Rita por fazer sentido quando mais nada faz. Pelas conversas da vida, gelados, karmas, e tudo o resto. Gracias.

Este trabalho não teria sido possível sem a ajuda e presença de todos vocês durante este ano. A tese que se segue é fruto da vossa amizade. Portanto, tudo isto também é vosso. Obrigado por tudo!

II. Abstract

Chlamydomonas reinhardtii is a unicellular, soil-dwelling green alga that has been the focus of several studies regarding photosynthesis and biodiesel production. When grown in specific conditions, such as sulphur or nitrogen (N) deficiency, this organism increases its H_2 production as well as triacylglycerol (TAG) synthesis, which occurs as a response to lower photosynthetic rates. In this investigation we characterize the phenotype of a *C. reinhardtii* mutant that performs a deficient CO_2 assimilation. This mutant, named I58W3, has three tryptophan amino acids replacing one isoleucine amino acid in Rubisco small subunit, close to Rubisco central channel.

Phenotypic characterization involved the growth of *C. reinhardtii* cultures under standard growth condition (N-replete) and N deprivation in TAP medium for 5 days. During the growth period cell number, dry weight, protein and chlorophyll contents and photosynthetic rates were measured. Lipid composition of *C. reinhardtii* cell lines was assessed through gas chromatography and thin layer chromatography, as well as Red Nile staining and subsequent spectrophotometry. Photosynthetic apparatus efficiency and integrity was also evaluated by pulse amplitude modulation (PAM) analysis. In order to compare Rubisco enzyme levels in control and I58W3 mutants, protein gel electrophoresis and immunoblotting were performed. Finally, quantitative PCR of several genes related to lipid metabolism and photosynthesis was performed in order to investigate transcriptional changes between I58W3 mutants and the control strain, under N-replete and N deprivation conditions.

Both protein and chlorophyll levels were affected under nitrogen deprivation as their concentration is lower in both control and mutant cells. Mutant cells appear to have a decreased photosynthetic efficiency and their photosynthetic apparatus does not function the same way as it does in control cells. Rubisco enzyme levels decrease in I58W3 cells and the expression of several genes, such as FAD or ω-13, is also lower in I58W3 cells in response to nitrogen deprivation.

Overall, I58W3 cells show a promising role in subsequent biodiesel production, since they show an increase in TAG lipid accumulation and decreased photosynthetic rates. Further genetic analyses of other genes, regarding different photosynthetic pathways, should be made in order to guarantee a thorough research and a complete database on I58W3 mutants.

Keywords: *Chalydomonas reinhardtii*, TAG, biodiesel, photosynthesis, Rubisco.

III. Resumo

Chlamydomonas reinhardtii é uma microalga modelo tendo sido usada para estudos da fotossíntese e do metabolismo energético dos lípidos. É o organismo eucariótico em que pela primeira vez foi possível modificar os genes das subunidades da enzima chave da fotossíntese, a ribulose-1,5-bisfosfato carboxilase/oxigenase (Rubisco). A enzima, além de assimilar o CO_2 atmosférico, também funciona como oxigenase, catalisando a primeira reação da via fotorrespiratória, o que a torna um ponto fundamental do metabolismo do carbono.

A Rubisco é uma das mais abundantes enzimas na antureza, com uma massa molecular total de 560 kDa. É constituída por 16 subunidades, 8 subunidades grandes (LSU, 55 kDa) e 8 subunidades pequenas (*SSU*, 15 kDa). Após a formação da enzima, as 8 subunidades grandes estão dispostas em dímeros em torno de um canal central que influencia a eficiência do centro catalítico, a especificidade CO2 / O2 e a estabilidade de toda a enzima. Contudo, pouco se sabe sobre a expressão génica e metabolismo energético dos lípidos em organismos com uma alteração profunda no canal central da Rubisco. A enzima também está presente no ciclo de Calvin-Benson, onde catalisa a primeira reação da via fotorrespiratória, o que o torna um ponto fundamental do metabolismo fotossintético do carbono. A síntese de Rubisco consome uma parcela substancial de recursos nutricionais de plantas e a sua degradação afeta a redistribuição de nutrientes dentro do organismo, o que significa que a Rubisco pode ter uma função de armazenamento em condições fisiológicas específicas, como falta de enxofre (S) ou azoto (N).

Um dos focos principais para o uso desta alga tem sido a sua capacidade de produzir H_2 e biodiesel, que ocorre especificamente em condições de stress ambiental, como por exemplo falta de azoto. Uma das consequências deste tipo de stress em *C. reinhardtii* é a síntese e acumulação de triacilglicerol (TAG), que é um precursor do biodiesel. Além disso outros processos como a fotossíntese e a produção/concentração de proteínas e clorofilas também sofrem alterações. Tendo tudo isto em conta, o foco desta investigação foi a caracterização fenotípica de um mutante de *C. reinhardtii*, I58W3, que na cadeia polipeptídica da subunidade pequena da Rubisco po*SSU*i uma mutação, três triptofanos (W) substituem uma isoleucina (I) na posição do resíduo aminoácido 58. Pelos estudos de cristalografia da Rubisco de *Chlamydomonas* o resíduo 58 localiza-se na entrada do canal central da estrutura da holoenzima. No presente foram realizados vários testes ao longo do crescimento das culturas controlo e I58W3 que visaram caracterizar este mutante a nível fotossintético, através de leituras da concentração de O_2 nas células e respetivas taxas fotossintéticas e de respiração, assim como leituras acerca da eficiência do aparelho fotossintético através de PAM; foram determinadas as concentrações de clorofilas e de proteínas ao longo do tempo das culturas em células mutantes e no respetivo controlo, bem como a monitorização do peso seco das culturas e do número de células ao longo dos cinco dias de crescimento; foi feita com detalhe uma análise da composição lipídica através de cromatografia gasosa e

cromatografia por camada fina, assim como leituras por espetrofotómetro de amostras das culturas coradas com Red Nile. Os níveis de Rubisco em I58W3 foram comparados com o controlo por eletroforese de proteínas e immunoblotting. Finalmente, alguns genes de interesse foram estudados, tentando comparar a sua expressão em células da cultura controlo com células da cultura I58W3. Adicionou-se mais um fator de comparação a este estudo, a carência de azoto no meio de cultura, por ser indutor da síntese de lípidos de reserva em microalgas.

Em situação de deficiência de azoto tanto o mutante I58W3 como o controlo diminuíram o teor de clorofila e de proteína. A nível fotossintético, comparando o controlo com o mutante I58W3, as taxas de fotossíntese foram menores para o mutante, o que indica alguma dificuldade na assimilação de CO_2 pela Rubisco, estando em linha com a mutação destas células. A análise por PAM também indica possíveis danos no aparelho fotossintético nesta estirpe mutante, o que também contribuirá para uma menor eficiência na produtividade. O mutante I58W3 mostra uma menor capacidade de absorção de energia quando comparado com o controlo, assim como valores inferiores de eficácia no transporte de eletrões e menos centros de reação. Além disso também apresenta valores mais acentuados de dissipação de energia sob forma de calor. A análise dos níveis da Rubisco mostram ser menores no mutante I58W3 do que no controlo, o que pode indicar também que esta estirpe não só tem dificuldades em assimilar eficientemente CO_2, como este fator é agravado pelo teor baixo da enzima Rubisco no cloroplasto das células de *C. reinhardtii*. Uma análise da composição lipídica leva-nos a crer que, como resposta das células a uma fotossíntese deficiente, ocorre uma alteração metabólica que provoca uma maior síntese e acumulação de lípidos, principalmente TAG. A análise genética, por qPCR, de genes relacionados com a síntese lipídica parece indicar que estes estão a ser expressos mais frequentemente na estirpe I58W3 do que em células controlo. Além disso, a expressão de um gene envolvido na fotossíntese também parece corroborar a hipótese de que este processo não é tão eficaz em I58W3.

Uma análise genética feita a amostras controlo e I58W3 a vários genes indica que as alterações a nível de acumulação de lípidos podem estar relacionadas com a síntese *de novo* destes, ou com uma menor síntese de dessaturases de ácidos gordos. O mutante I58W3 apresenta maior expressão de *DGAT1*, uma proteína envolvida na síntese de TAG, que o controlo, sendo que esse aumento é mais acentuado em condições de deficiência de azoto. Este mutante também apresenta valores de expressão de *CrDES* inferiores ao controlo, o que nos indica que existe uma acumulação de ácido linoleico em detrimento de ácido pinolénico em I58W3. A proteína $cytb_6f$ encontra-se mais expressa em I58W3, embora a eficiência fotossintética deste seja menor que a do controlo. A síntese da hidrogenase *HydA1* não varia significativamente em I58W3 independentemente da presença ou ausência de azoto. Os resultados obtidos permitem-nos concluir que, dos genes estudados, existem diferenças a nível da sua expressão devido à mutação em conjunto com a deficiência de azoto. Por outro lado a síntese de proteínas como a hidrogenase *HydA1* ou a galactolipase *PGD1* parecem não mudar com a mutação.

O fato de que esta estirpe consegue acumular lípidos neutros como resposta às consequências da sua mutação, assim como à deficiência de azoto, é fulcral no âmbito da temática proposta.

A produção de biodiesel seria então possível utilizando estas algas em conjunto com um meio cuja característica principal seria a falta de azoto. A união destes dois fatores poderá tornar possível no futuro culturas cujo objetivo é a produção de biodiesel.

Palavras-chave: *Chlamydomonas reinhardtii*, TAG, biodiesel, fotossíntese, Rubisco

Index

Figure/ Table List

cells cultures, and results were normalized per 10^6 cells. Values correspond to average ± standard error, n=3; asterisks indicate significant differences ($p \leq 0.05$).

3.7 - Fatty acid composition of S1-Wt and I58W3 in N-replete and N deprived media at 48 h. Values correspond to average ± standard error, n=3; asterisks indicate significant differences ($p \leq 0.05$).

3.8 – Total mg FA/g DW of S1-Wt control and I58W3 *C. reinhardtii* strains under N repletion (N 100%) or depletion (N 5%). Measurements were made at 48h of culture growth. Values correspond to average ± standard error, n=3; asterisks indicate significant differences ($p \leq 0.05$).

3.9 – TAG percentage in control (S1-Wt) and mutant (I58W3) strains in N-replete (N100) or deplete (N5) media. Measures were made with samples with 48h of cell growth and analysed through thin layer chromatography followed by gas chromatography.

3.10 – Photosynthetic/respiratory ratio at 48h and 96h of *C. reinhardtii* control strain (S1-Wt) and mutant strain (I58W3) in normal TAP medium (100% N) and with deficient nitrogen regime (5% N). Values correspond to average ± standard error, n=3; asterisks indicate significant differences ($p \leq 0.05$).

3.11 – Phenomenological energy fluxes in *C. reinhardtii* grown at 48 °C (upper graphic) and 96 h (lower graphic) under N-repletion or depletion. Absorbed energy flux per cross-section (ABS/CS); Trapped energy flux per cross-section (TR/CS); Electron transport energy flux per cross-section (ET/CS); dissipated energy flux per cross-section (DI/CS). Reaction Centres per cross section (RC/CS).

3.12 – Fold change in gene expression calculated using Livak method. Actin was used as the control housekeeping gene. Values correspond to average ± standard error, n=3; asterisks indicate significant differences ($p \leq 0.05$). Fatty acid desaturase (*CrDES* and *CrFAD6*), galactolipase (*PGD1*), diacylglycerol acyltransferase (*DGAT1*), hydrogenase (*HydA1*), Rubisco small subunit (*SSU*) and $cytb_6f$ protein.

Table 1 – Dry weight (DW) and chlorophyll levels of *C. reinhardtii* cells, wild-type control (Wt-S1) and I58W3 mutant strain grown in Tris-acetate phosphate (TAP) under nitrogen-replete (100% N) or nitrogen-depleted (5%N) conditions, at 48 and 96 hours. Values correspond to average ± standard error, n=3; asterisks indicate significant differences ($p \leq 0.05$).

Table 2 - PAM-derived parameters obtained from *C. reinhardtii* grown at 48 h and 96 h under N-repletion or depletion. Number of reduction turnovers (oxidation and re-reduction of Q_A) (N); Efficiency with which an absorbed photon results in electron transport beyond Q_A- (ΦEo); Efficiency or probability with which a PSII trapped electron is transferred from Q_A to Q_B (ΨO); Density or amount or concentration of RCs per absorption energy flux (RC/ABS); Absorbed energy flux per reaction centre (ABS/RC); Trapped energy flux per

reaction centre (TRo/RC); Electron transport flux per RC (ETo/RC); Quantum yield of energy dissipation as heat (ΦDo); Proportion of electron transport to energy dissipation as heat (Et_O/Di_O). Values correspond to average, n=3; asterisks indicate significant differences ($p \leq 0.05$).

Table 3 – Rapid Light Curve parameters in 48 and 96 h old samples of *C. reinhardtii* under N deprivation and N repletion. Values correspond to average of n = 3 samples. Marked (*) values indicate significant differences between mutant, S1 N5 and S1-Wt N100 control strains ($p \leq 0.05$). α (photosystem II efficiency), ETR_{max} (maximum relative electron transport), β (photoinhibition parameter). Values correspond to average, n=3; asterisks indicate significant differences ($p \leq 0.05$).

Abbreviation/Acronym list

ATP – Adenosine triphosphate

$cytb_6f$ – Cytochrome b_6f complex

CCM – Carbon concentration mechanism

DAG – Diacylglycerol

FA – Fatty acid

FFA – Free fatty acids

GC – Gas chromatography

LSU – Rubisco Large subunit

MGDG - Monogalactosyldiacylglycerol

NADP - Nicotinamide adenine dinucleotide phosphate

OJIP – Chlorophyll fluorescence analysis test

PAM – Pulse amplitude modulation

PS – Photosystem

PVDF – Polyvinylidene difluoride

Q_A – Quinone A

Q_B – Quinone B

qPCR – Quantitative polymerase chain reaction

RC – Reaction Centre

RLC – Rapid Light Curve

RN – Red Nile

Rubisco – Ribulose -1,5- bisphosphate carboxylase/oxygenase

RuBP – Ribulose-1,5- bisphosphate carboxylase

SDS-PAGE - Sodium dodecyl sulphate polyacrylamide gel electrophoresis

SSU – Rubisco small subunit

TAG – Triacylglycerol

TAP – Tris-acetate-phosphate

TBS – Tris buffer saline

TLC – Thin layer chromatography

TTBS – Tween + TBS

1. Introduction

1.1. Chlamydomonas reinhardtii as a model organism

Chlamydomonas reinhardtii is a 10 µm diameter unicellular, soil-dwelling green alga (Fig. 1.1). Its genome is fully sequenced and has a size of 121 Mb, corresponding to 17 chromosomes. It has several mitochondria, two anterior flagella with motility and reproduction purposes and a single chloroplast that holds the photosynthetic apparatus and critical metabolic pathways (Merchant *et al*., 2007). Its wild type has a cell wall that contains hydroxyproline-rich glycoproteins and is composed by 7 layers. Cell-wall deficient mutants were isolated and widely used for genetic engineering. The single cup shaped chloroplast occupies a large part of the cell. Inside the chloroplast is the photosynthetic apparatus, the eyespot which allows orientation according to light sources, the pyrenoid which functions as a CO_2 concentration mechanism (CCM) and where the enzyme ribulose-1,5-bisphosphate carboxylase/oxygenase, Rubisco (EC: 4.1.1.39), is present in high concentrations. Inorganic carbon carriers responsible for seizing carbon in the form of HCO_3^- and carbonic anhydrases are involved in this mechanism of micro compartmentation, which converts the bicarbonate ion to CO_2. Thus, there is a decrease in the loss of carbon dioxide (its concentration is about 40x higher than the atmospheric concentration), which is then fixed by Rubisco, initiating the Calvin cycle (Harris, 2001; Meyer and Griffiths, 2013).

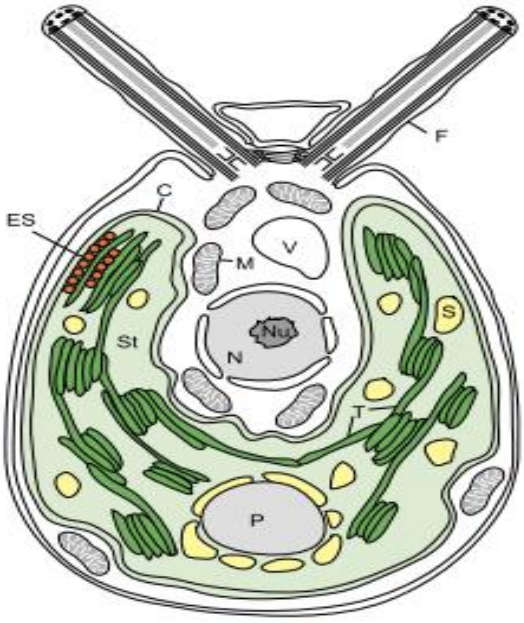

Figure 1.1. *Chlamydomonas reinhardtii* cell morphology (Dent *et al.*, 2001).

N – nucleus; Nu – nucleolus;
M – mitochondria; C – chloroplast;
V – vacuole; T – thylakoid membranes;
S – starch grain; P – pyrenoid; St – stroma;
ES – eye spot; F - flagella

The model algae *C. reinhardtii* is considered to be useful for photosynthesis and chloroplast biogenesis studies as it is able to grow in several environmental conditions such as total light absence or the presence of an organic carbon source, such as acetate, keeping its photosynthetic device functional. In this situation, mutant strains of easy transformation whose photosynthetic apparatus is compromised also show growth in heterotrophic and mixotrophic conditions. The wild type strain is grown in liquid or solid medium at neutral pH, at an optimal temperature of 25 ^{O}C. Both in mediums with acetate and in minimal mediums, the wild type grows better in the presence of light, a doubling time of 6-8 h *(*Dent *et al.*, 2001; Harris, 2001; Merchant *et al.*, 2007). *C. reinhardtii* is also used in the production of molecular hydrogen, a non-polluting alternative energy source with a low production cost and without the need to use cultivated land. This microalgae uses solar radiation to reduce free protons to H_2 through a set of reactions catalysed by two reduced ferredoxin-dependent hydrogenases. Biofuel production only occurs under anaerobic conditions, as the transcription and activity of the hydrogenases is inhibited by oxygen which is released during photosynthesis (Happe and Kaminski, 2002). On the other hand, some strains of *C. reinhardtii* with certain mutations in the Rubisco enzyme have been studied in this context, since their low photosynthetic rates increase H_2 production (Rupprecht, 2009; Pinto *et al.*, 2013;).

Another biotechnological application of this algae is bioremediation. *C. reinhardtii* can be used in the treatment of wastewater rich in nutrients and heavy metals which are hazardous to human health (Tsekova *et al.*, 2010). Therefore this algae may be one of the solutions to solve this problem because not only it consumes the existing nutrients and uses them to increase its biomass but it also absorbs and accumulates heavy metals in its cell wall and vacuole (Hasan *et al.*, 2014; Zeraatkar *et al.*, 2016)

In addition, this microalga is studied for its potential in the production of precursors of biodiesel (triacylglycerol, TAG), which is a renewable and biodegradable fuel. In stress conditions the metabolism of *C. reinhardtii* is affected and could induce accumulation of TAG, which are formed by a glycerol molecule linked to three fatty acids (FAs). The response to N deficiency changes the life cycle from vegetative to reproductive and steers *C. reinhardtii* metabolism towards a path that stimulates a higher accumulation of storage compounds to prepare for zygote formation (Johnson and Alric, 2013). N deprivation can also decrease the efficiency and subsequent number of PSII complexes available during photosynthesis, as well as inducing the expression of nitrogen uptake genes (Miller *et al.*, 2010; Park *et al.*, 2015) as well as lipid metabolism genes (Boyle *et al.*, 2012).

1.2. Photosynthesis and Rubisco

Photosynthesis is a unique process since it is through it that photosynthetic organisms synthesize organic compounds from solar energy, and is modulated by several environmental factors such as temperature, drought, CO_2 concentration as well as quality and quantity of light (Minagawa and Tokutsu, 2015). Photosynthesis is divided in two major stages. Photochemical reactions, which depend directly on light, and chemical reactions that occur in the Calvin-Benson cycle (fig. 1.2) (Taiz and Zeiger, 2014).

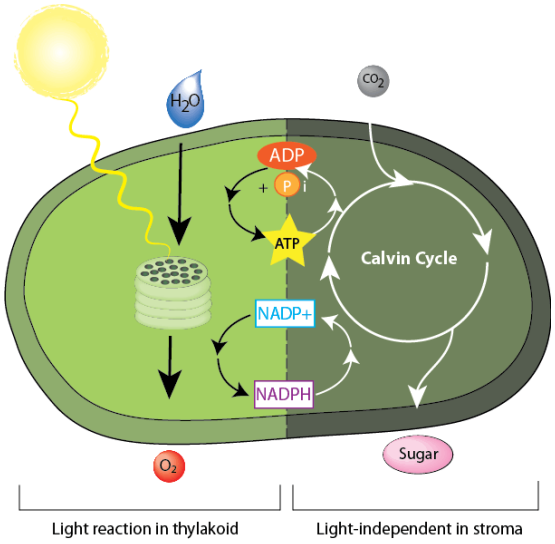

Figure 1.2. Light dependent and independent reactions in photosynthesis.

Source: adapaproject.org

In the chemical phase, which occurs in the chloroplast stroma, the reactions through which CO_2 is fixed and the carbon is reduced in the Calvin-Benson cycle. In the first step, CO_2 enters the Calvin-Benson cycle by reacting with ribulose-1,5-bisphosphate, forming two molecules of 3-phosphoglycerate. The reaction is catalysed by the Rubisco enzyme (ribulose-1,5-bisphosphate carboxylase/oxygenase.

Rubisco is one the core factors of CO_2 entrance into the biosphere is the enzyme ribulose-1,5-bisphosphate carboxylase/oxygenase (E.C. 4.1.1.39), Rubisco (Fig. 1.3). Its low affinity towards atmospheric CO_2 and the use of O_2 as an alternate substrate for the competing process of photorespiration make Rubisco an inefficient initial CO_2 fixing enzyme of the photosynthetic process. Subsequently, land plants must assign as much as 50% of their leaf nitrogen (N) to Rubisco, making this specific enzyme one of, if not the most abundant enzymes in the world (Ellis, 1979). In *C. reinhardtii* and many other species the CCM mechanism counters Rubisco low atmospheric CO_2 affinity and creates a higher concentration of CO_2 around the enzyme (Giordano *et al.*, 2005; Jungnick *et al.*, 2014).

Rubisco is one of the largest enzymes in nature, having a total molecular mass of 560 kDa. It consists of 16 subunits, 8 large subunits (LSU, 55 kDa) and 8 small subunits (*SSU*, 15 kDa). In plants and green algae, the large subunits of this enzyme are encoded in the rbcL gene from the

chloroplast genome and the small subunits are encoded by a family of nuclear genes called rbcS. After the translation process that occurs in the cytoplasm the polypeptides from the small subunits are imported into the chloroplast, where they associate with large subunits through the action of a chaperone and then form the Rubisco holoenzyme (Spreitzer and Salvucci, 2002). After the enzyme is formed the 8 large subunits are arranged in dimers around a central channel with each dimer having two active centres where the substrates are bound. The 8 small subunits are arranged in two tetramers that bind to the large subunits poles. Small subunits show greater divergence between species than large subunits, especially in the loop between β-A and β-B chains. This loop forms the entrance of the Rubisco central channel and establishes contact between the small and large subunits, influencing the efficiency of the catalytic centre, CO_2/O_2 specificity and the stability of the whole enzyme (Spreitzer and Salvucci 2002; Esquível *et al*., 2006;).

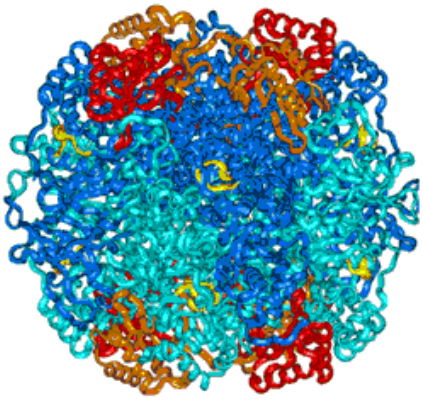

Figure 1.3. Rubisco three dimensional model highlighting 8 large subunits (Blue) and 8 small subunits (Red and Orange). Source: ars.usda.gov

Rubisco synthesis consumes a substantial portion of plant nutrient resources and its degradation impacts the redistribution of nutrients within the organism, which means that Rubisco can have a storage function under specific physiological conditions, such as sulphur (S) or N starvation (Esquível *et al.,* 2000), and these features allow for the acclimation of an organism to external environmental conditions. Recently, since Rubisco has a predominant role in the photosynthetic metabolism, Rubisco mutants have been studied with the aim of finding biotechnological applications. For instance, the mutant Y67A in *C. reinhardtii*, where the tyrosine aminoacid (Y) of position 67 of Rubisco small subunit was replaced by an alanine aminoacid (A), has the ability to boost its H_2 production because it presents a reduced photosynthetic rate due to the lack of stability of the Rubisco enzyme induced by the targeted mutation (Pinto *et al*., 2013;) (fig. 1.4). This mutant also produces high concentration of neutral lipids, making it a potentially important strain for biodiesel production (Esquível *et al.*, 2017).

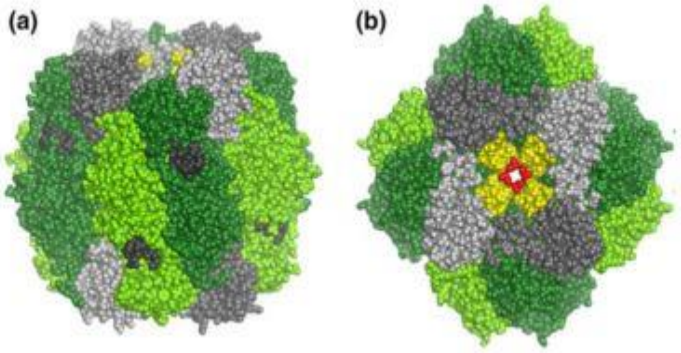

Figure 1.4. X-ray structures of Rubisco holoenzymes (Esquível *et al.,* 2013). (a) *Chlamydomonas* Rubisco side view. (b) *Chlamydomonas* Rubisco top view. The small-subunit residue that defines the narrowest diameter of the central solvent channel is coloured red, and is where the mutation has its effect (*Chlamydomonas* Ile-58).

1.3. Lipids Metabolism in *C. reinhardtii*

Nutrient limitation is an essential trigger for triacylglycerol TAG accumulation in algae, and N deprivation is considered to be one of the best (Rodolfi *et al.*, 2009; Schmollinger *et al*., 2014). When N deprivation is carried out on a culture, photosynthetic rates are negatively affected and carbon fixation is diverted from protein synthesis to carbohydrate or lipid synthesis, and it is believed that increases in lipid content during N deprivation are mainly obtained at the expense of other components, particularly starch (Rodolfi *et al*., 2009). While carbohydrates can reach above 70% of the dry biomass with no reduction in productivity, lipid accumulation is often associated to a reduction in biomass productivity. However, there are also suspicions that cellular lipid accumulation during N deprivation may derive from newly fixed carbon in certain green microalgae. The ability for *de novo* lipid synthesis seems a characteristic of some oleaginous microalgae, which, when grown under N deprivation channel the excess of carbon and energy into storage lipid (mainly TAG). This can due to the fact that TAG do not contain N atoms and their accumulation diverts carbon toward storage in situations where carbon cannot be used for cell growth and division. *C. reinhardtii* has been as a reference organism for understanding TAG biosynthesis under N deprivation (Fernandez and Galvan, 2008; Wang *et al*., 2009; Miller *et al*., 2010; Boyle *et al.*, 2012; Blaby *et al.*, 2013) . Nevertheless, the signalling pathways that affect these metabolic changes are not yet understood and therefore cannot be manipulated in order to control carbon movement toward TAG for the biodiesel industry. *C. reinhardtii* can utilize a number of different N sources, both inorganic, such as nitrate, nitrite, and ammonium, and organic, such as urea and amino acids, although ammonium is preferred (Florencio and Vega, 1983). N deprivation has been commonly used as a standard condition to increase neutral lipid accumulation in several microalgal species (Thompson, 1996; Merzlyak *et al*., 2007; Hu *et al*., 2008; Philipps *et al*., 2011). Upon certain environmental stresses, particularly nutrient shortage, various algae including *C. reinhardtii* accumulate energy-rich storage compounds such as starch and TAG (Guschina and Harwood, 2006; Hu *et al*., 2008; Rodolfi *et al*., 2009; Wang *et al*., 2009; Siaut *et al*., 2011). Increases in lipid content of up to 70% of the dry biomass have been reported in several species in response to limiting N supply in batch cultures, with TAG mainly containing saturated and monounsaturated fatty acids, which form the majority of the lipid fraction in the starved cells (Borowitzka and Borowitzka, 1988; Roessler, 1990). Esquível *et al.* (2017) show that *C. reinhardtii* Rubisco small subunit mutants display an increase in neutral lipids, such as TAG, over polar lipids. However, some inconsistencies are found in the response to N deprivation. Diatoms, which usually have a relatively high exponential-phase lipid content, do not respond to N deprivation by increasing their lipid content (Shifrin and Chisholm, 1981). Green microalgae have been reported to show a range of responses, from several fold increases from exponential-phase values in *C. pyrenoidosa*, to no changes or even a slight reduction in some *Dunaliella spp*. and in *Tetraselmis suecica* (Borowitzka and Borowitzka, 1988). The response to N deprivation in *C. reinhardtii* however seems to be consistent in that this species is able to accumulate significant amounts of TAG under N deprivation (Wang *et al*., 2009; Siaut *et al*., 2011). As part of their lipid composition, *C. reinhardtii* are also characterized by the presence of ω-3 fatty acids.

1.4. Objectives

In this study we have performed a phenotypic characterization of the I58W3 *C. reinhardtii* mutant that has three tryptophan (Trp) residues, which replace an isoleucine amino acid in position 58 of Rubisco small subunit amino acid chain, close to the entrance of the central channel of the Rubisco enzyme (Taylor *et al*., 2001). It was found that this mutation caused a deficient CO_2 assimilation due to a great decrease in the carboxylation rate of Rubisco compared with the control strain (Esquível *et al,* 2013). It seems worth to investigate if this "critical" mutation could have effects reaching the photochemical reactions of photosynthesis, respiration rates and the carbon routes for lipid accumulation. Since *C. reinhardtii* is able to accumulate significant amounts of storage lipids particularly under N deprivation, comparative analyses were undertaken with mutated cells grown in mixotrophic conditions in TAP – Tris, acetate phosphate medium and in N-deficient conditions in order to assess the effects of the I58W3 mutation alongside the environmental N deficiency in lipid metabolism, photosynthesis, protein and chlorophyll production, cell growth and biomass levels. Genetic analyses were performed to understand the role of specific genes tied to the cells metabolism. Target genes consisted of a housekeeping gene (Actin), hydrogenase, Rubisco small subunit, *DGAT1* which is involved in *de novo* synthesis of TAG (Chen and Smith, 2012), cytb6f, a protein complex involved in photosynthesis, *CrDES* and *CrFAD6*, fatty acid desaturases important in TAG synthesis (Sato *et al*., 1997; Kajikawa *et al*., 2006; Li-Beisson *et al.*, 2015) and *PGD1*, a galactolipase (X. Li *et al.*, 2012).

2. Materials and methods

2.1. Cell strains and cell culture growth

Two wall-less *C. reinhardtii* lines, kindly provided by Dr. Robert Spreitzer, USA, were used. The parental line served as the control strain (S1-Wt) and the genetically altered line had a targeted mutation, where 3 tryptophan aminoacids replaced an isoleucine aminoacid in position 58 of Rubisco small subunit (I58W3). Cell stocks were maintained in solid Tris-Acetate-Phosphate (TAP) media containing agar and transferred periodically to new TAP media to guarantee their viability.

Both cell lines were grown simultaneously and were kept in 250 mL Erlenmeyer flasks in constant lighting (35 $\mu mol.m^2.s^{-1}$) and agitation (120 rpm, Agitorb 200 IC) to guarantee oxygen circulation and nutrient homogeneity. Five days after inoculation N-deprivation was imposed (N 5%) (supplement 1) (Philipps *et al.*, 2011) to S1-Wt and I58W3 strains. Each 1 L flask contained 255 mL of media and 45 mL of the inoculated cell culture. This transfer was done by centrifuging 45 mL of the inoculation culture (5 minutes at 500 *g*, Allegra 25R Centrifuge, Beckman Coulter) then adding 60 mL of the corresponding media to the pellet, homogenising it and adding it to the assigned Erlenmeyer flask.

2.2. Dry weight and cell counting

Spot tests were performed to characterize the growth of both strains in mixotrophic, heterotrophic and autotrophic conditions. Equal number of cells were plated on TAP medium in the light (under the intensity of 35 $\mu mol.m^2.s^{-1}$), in the dark and on minimal medium in the light. The cultures were maintained at 25ºC.

Dry weight was determined using 45 mL of cell cultures after centrifugation for 5 minutes at 500 *g*, removal of the cell culture and incubation at 80º C for a week in pre-weighted falcon tubes. Cell counts were made daily during five days after the transfer to new media, in a Neubauer chamber using a Leitz Dialux 22 microscope at 100x magnification, using 20 µL of cell culture.

2.3. Pigments analyses, extraction and quantification

Chlorophyll contents were determined using 1 mL of cell culture. After centrifugation for 5 minutes at 7500 *g* in the Mini Spin Plus (Sigma) cells were resuspended in 1 mL of 100% (v / v) methanol and stored for one day at 4 ºC in the dark. The absorbances at 652.4 and 665.2 were read in a Shimadzu UV-2100 spectrophotometer. Chlorophyll *a* and *b* contents were calculated according to Lichtenthaler (1987) (supplement 2).

2.4. Protein extraction and quantification

To measure protein content 2 mL samples were taken from each of the liquid cultures to eppendorf tubes. Samples were centrifuged for 4 minutes at 7500 *g* in the Mini spin Plus (Sigma) centrifuge to concentrate the cells and remove the culture medium. Cells were

resuspended in 150 µL of sample buffer (taken from a 60 µL β-mercaptoethanol + 940 µL Laemmli sample buffer solution). Samples were then heated to 98º C for 3 minutes and stored at -20º C. Dilutions of bovine serum albumin were used to prepare a series of protein standards. Protein measurements were made by following Lowry analysis using Folin phenol reagent using a modified method (Bensadoun and Weinstein, 1976).

2.5. Oxygen electrode measurements

The oxygen electrode (Clark-type electrode) is formed by 2 electrodes immersed in an electrolyte solution. Both oxygen electrode discs have a platinum cathode and a silver anode. (fig. 2.1). The electrodes are protected by a thin Teflon membrane which is permeable to oxygen. When a voltage of 700 mV is applied oxygen is reduced at the platinum surface, initially to hydrogen peroxide (H_2O_2) and electrons are donated to oxygen which acts as an electron acceptor (Walker, 1987).

2 mL samples of each culture were used to determine the oxygen production and consumption rates. Samples were placed in the electrode chamber (Hansatech Instruments, Oxytherm) after its calibration and were maintained in constant agitation. The measurements were made in two phases, with the cells exposed to light, produced by a projector lamp with an intensity of 100 µmol m^{-2} s^{-1} and without being exposed (dark phase), as to mimic photosynthetic and respiratory conditions, respectively. Each measurement lasted around 20 minutes, each with light and dark cycles of 5 minutes. Net photosynthesis and respiration rates were then estimated from the maximum slopes of the curves.

2.6. Pulse amplitude modulated (PAM) fluorometry

PAM fluorometry functions on a basic signal modulation in which light is delivered in a series of signal pulses. This method can be used in photobiology and can obtain spectrofluoromic measurements of the kinetics of fluorescence by measuring the increases and decay of the light harvesting antennae of the thylakoid membranes (Maxwell and Johnson 2000). PAM fluorometry provides a fast assessment of the overall photosynthetic state through comparison of photosynthetic rates based on fluorescence. Specifically, the measurement of fluorescence is often used as an indicator of the early effects of stress on autotroph photosystems caused by varying environmental conditions.

Chlorophyll transient light curves were assessed by the OJIP test. The OJIP test is based on the theory of energy flow in thylakoid membranes, therefore facilitating a better understanding of relationships between the biophysical side of photosynthesis and the fluorescence signals (Chernev *et al.*, 2006). This test test also provides insight on the probability of the fate of absorbed light energy as well as detailed information on photosynthetic apparatus structure and function (Kalaji *et al.*, 2011). The O level represents all the open reaction centres (RC) at the onset of illumination with no reduction of quinone a (Q_A) (the fluorescence intensity lasts for 10 ms). The rise of transient fluorescence from O to J shows net photochemical reduction of Q_A, which is the stable primary electron acceptor of PSII, to Q_{A-} (that lasts for 2 ms). Then, the phase from J to I was due to reduced states of closed reaction centres (RC) such as Q_{A-} Q_{B-}, Q_A Q_{B2-} and Q_{A-} Q_B H_2 (lasts for 2-30 ms). The P level (300 ms) coincides with maximum

concentration of Q_{A-} Q_{B2} with plastoquinol pool maximally reduced. This P reflects an equilibrium between light incident at the PSII side and the rate of utilization of the chemical (potential) energy and the rate of heat dissipation (Zhu et al. 2005). Rapid Light Curves (RLC) were achieved using the pre-programmed light curve (LC1) protocol which performs successive measurements of the sample photosystem II efficiency (ϕPSII) under various light intensities (20, 50, 100, 200, 300 and 500 µmol photons m^{-2} s^{-1}) of continuous illumination relating the rate of photosynthesis to photon flux density (PAR). A list of parameters evaluated by PAM fluorometry is available in supplement 3.

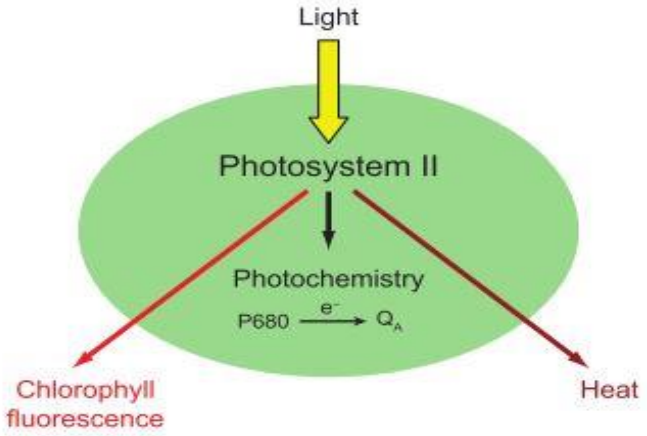

Figure 2.1. Representation of harvested lights 3 possible paths. The light energy absorbed by chlorophylls associated with the PSII can be used to trigger photochemistry where an electron (e−) is transferred from reaction centre chlorophyll, P680, to the primary quinone acceptor of PSII, Q_A. Otherwise, absorbed light energy could be lost as chlorophyll fluorescence or heat. Source: Baker, 2008.

PAM chlorophyll fluorescence measurements were performed using a FluoroPen FP100 (Photo System Instruments, Czech Republic) on samples using a 1 mL cuvette. All fluorometric analysis were carried out at the end of the experimental period in dark-adapted samples.

2.7. Nile Red fluorescence

Spectrofluorometric analyses were performed with Red Nile (a dark-purplish-red dye) for lipids semi-quantitative measurements in cell cultures. 1 mL samples of each culture were taken and their fluorescence was read in a Bio-Tek Synergy HT spectrophotometer, in two different ways: with and without Red Nile dye dissolved in methanol (1 µg/mL). Samples were excited at a wavelength of 460 nm and emission spectra acquired over the range of 645 nm. Relative TAG content was calculated by subtracting the fluorescence without the dye (chlorophyll fluorescence intensity) to the fluorescence levels with the dye, where Red Nile highlights TAG fluorescence (Alemán-Nava *et al*,. 2016).

2.8. Lipid extraction, methylation and gas chromatography (GC) analysis

Lipid extraction was made according to Bligh and Dyer (1959), where lipids were extracted in the chlorophorm phase while other cell components remain in the interface or in the aqueous phase. Lipases were inactivated at 100 ºC for 3 minutes and the lipid extracts are stored under N atmosphere, preventing lipid degradation by oxygen.

Cell pellets corresponding to 45 mL cultures were suspended in 1 mL of boiling water and incubated at 100 ºC for 3 minutes. The suspension was then transferred to a mortar where it was homogenised and transferred to a glass tube. The mortar was successively washed with 7 mL of methanol, chlorophorm and 6 mL of water, which were added to the same glass tube. After vortexing, the extract was centrifuged for 5 minutes at 4000 *g*. The organic (lower) phase was recovered with a Pasteur pipette to another tube and was evaporated at 37º C under N atmosphere. The lipid residue was resuspended with 100 µL of ethanol-toluene solution (1/4 v/v), or 1 mL for thin layer chromatography, and preserved under N atmosphere at -20º C.

In order to obtain methyl esters, lipid saponification (fatty acid cleavage) and methylation are simultaneously performed by using methanol and sulphuric acid. The fatty acid methyl esters (FAME) can then be used in gas chromatography (GC) analyses. In this procedure 20 µg of margaric acid (heptadecanoic acid, or C:17, internal standard) were added 100 µL of total lipids and the solvents evaporated under N_2 atmosphere. Three mL methanol sulphuric acid (2.4% H_2SO_4 in methanol (v/v)) were added for 1 hour at 70º C. After cooling, the resulting methyl esters are recovered by adding 3 mL of petroleum ether and 2 mL of water, followed by vortexing and centrifuging (5 minutes at 4000 *g*). The upper phased was transferred to another tube and evaporated at 37 ºC under N atmosphere.

The FAME were then suspended in 50 µL of hexane to allow GC analysis (430 Gas Chromatograph, Varian). The chromatograph was equipped with a hydrogen flame ionization detector set at 300 °C. The temperature of the injector was set to 270 °C, with a split ratio of 50. The fused-silica capillary column (50 m x 0.25 mm; WCOT Fused Silica, CP-Sil 88 for FAME; Varian) was maintained at a constant nitrogen flow of 2.0 mL/min and the oven temperature set at 190 °C. Fatty acid separation was made for 7 minutes. Fatty acid quantification was assessed through their peak area by comparing it with C17 area. Data analysis was done through the Galaxie software.

2.9. Thin layer chromatography (TLC)

Different lipid classes are separated by TLC, allowing the separation between polar lipids, including galactolipids and phospholipids, and neutral lipids including free fatty acids (FFA) diacylglycerol (DAG) and TAG. Samples were applied at the base of a silica gel plate (G 60, Merck) and separated using a solvent system developed by Mangold (Wagener 1965). *Arabidopsis thaliana* leaf lipids were used as standards for comparison with *C. reinhardtii* lipids. After the solvent evaporation the plate was sprayed with primuline (0.1% in acetone 80%) and observed under UV light. Each lipids classes were then scraped into tubes containing the internal standard and methylated as above described (2.7) before GC analysis.

2.10. Protein electrophoresis

One dimensional gel electrophoresis is a technique that offers information about proteins molecular size, quantity and overall purity. It is also usually the first step in immunoblotting and immunodetection (Gallagher, 2012).

Sodium dodecyl sulphate polyacrylamide gel electrophoresis (SDS-PAGE) is currently the most used electrophoresis technique. At the pH at which gel electrophoresis is carried out the SDS molecules are negatively charged and bind to proteins in a fixed ratio, approximately one molecule of SDS for every 2 amino acids (Bhuyan 2010; Ninfa *et al*., 2010). This way, when a current is applied to the gel, proteins migrate to the positive charge electrode. Due to gel matrix properties proteins with a lower mass migrate faster than higher mass proteins (Hames, 1998).

Sample preparation - 2 mL samples were collected from the liquid cultures. The cells were sedimented by centrifugation (7500 *g* for 4 minutes) with Mini spin Plus (Sigma) centrifuge and resuspended in 125 mM Tris HCl (pH 6.8) with 4% (w/v) SDS, 20% (v/v) glycerol, 10% (v/v) 2-mercaptoethanol, 0.004% (w/v) bromophenol blue (Laemmli solution). Samples were then heated to 98º C for 4 minutes to promote cell lysis and protein denaturation. The samples were stored at -20º C. Discontinuous SDS-PAGE (10% polyacrylamide in the resolving gel and 5% in the stacking gel) were prepared using Bio-Rad Mini-PROTEAN Tetra cell cassettes. Samples were loaded into the wells and the gel was run at a constant 200 V for 1 hour. Protein bands were stained with 0.1% (w/v) Coomasie Brilliant Blue R-250 in 20% methanol and 5% acetic acid.

2.11. Immunoblotting

Immunoblotting, or western blotting, is an assay used for the detection and characterization of proteins by taking advantage of the inherent specificity in antigen-antibody recognition, since it involves electrophoretic separation of lipopolysaccharides, proteins or glycoproteins by gel electrophoresis, which is followed by transfer and binding to nitrocellulose, polyvinylidene difluoride (PVDF), or nylon.(S. Gallagher and Chakavarti, 2008; Mahmood and Yang, 2012).

After protein electrophoresis the gel's contents were transferred to a PVDF membrane by using transfer buffer (25 mM Trizma base, pH 8.3, 192 mM Glycine, 20% methanol (v/v)) The transfer was performed overnight at a constant 20 V.

Ponceau dye was used to check if the transfer had been successful. The membrane was developed using the buffer Tris-saline/Tween 20% TTBS (100 mM Trizma base, 0,9% (w/v) NaCl, 0.1% (v/v) Tween 20 pH 7.5), a primary rabbit antibody raised against LSU-Rubisco (1:1000 dilution) and a secondary goat anti-rabbit IgG antibody coupled to horseradish peroxidase (Bio-Rad catalogue no. 170-6515) in a 1:2000 dilution. The revealing solution 4-chloro-1-naphtol in 5 mL methanol. Gel-Doc Quantity One from Bio-Rad was used for image analysis.

2.12. Gene expression analysis by qPCR

Gene expression was studied in cells collected 48 h after the beginning of the N limitation treatment. Cells were collected by centrifugation (5 minutes at 500 *g*), immediately frozen in liquid N_2 and stored at -80 ºC. RNA extraction was then done with the RNeasy Mini kit (Qiagen) according to the manufacturer instructions, with freeze and thaw cycles of samples in the initial phase of the protocol. RNA concentration and purity was assessed using a Thermo Fisher Scientific NanoDrop 1000, where a ratio of 2 is usually considered pure for RNA (Matlock, 2012). RNA purity of gathered samples were reported between 2.10 and 2.15. RNA integrity was checked by agarose gel electrophoresis (1% agarose in tris acetate EDTA (TAE) buffer) using a Bio-Rad Mini-Sub Cell GT cell and PowerPac Basic power supply. After migration results were observed under UV light in a Bio-Rad Molecular Imager Gel Doc XR Imaging System.

cDNA was synthesized using Nzytech NZY M-MuLV First-Strand cDNA Synthesis Kit. qPCR protocol was then applied, using a Bio-Rad iTaq Universal SYBR Green Supermix, in order to assess gene expression of several target genes and compare their expression between the samples. qPCR consisted in an initial 3 minute heating phase of 95º C, 40 cycles of denaturation and annealing/extension (10 seconds at 95º C and 30 seconds at 60º C) and a melting curve phase of 0-5 ºC increases from 55 to 95 ºC (in a Bio-Rad MiniOpticon Real-Time PCR System). Primers used are shown in supplement 4. Fold change in gene expression between samples was calculated by the Livak method (Livak and Schmittgen, 2001).

2.13. Statistical analysis

Taking into account the objectives of the study, we considered the application of the Paired samples t-Test. Due to the small number of replicates *per* test (n = 3), which prevented the normality in all samples, t-test was then replaced by a non-parametric test, the Wilcoxon Signed-Ranks test. Using this we then proposed the following hypothesis:

H0: There are no differences between the median of the samples

H1: There are differences between the median of the samples

Statistical analysis was then performed using the Statistical Package for the Social Sciences (SPSS). Significant differences take into account a p-value ≤ 0.05.

3. Results/Discussion

3.1. Changes in cell metabolism

In order to clarify the effect of the closure of the Rubisco central channel on cell growth, the mutant I58W3 were grown in different N concentrations and the growth compared with the control (S1-Wt). Colour differences between cultures are shown in fig. 3.1.

Cells were grown in N-depleted and N-replete liquid media. Table 1 shows the culture dry weight (DW) and the chlorophyll levels (chlorophyll *a*, *b* and total chlorophyll) at 48 and 96 h of culture growth. 5% N negatively affects growth. Comparing both strains at 48 h it is possible to see that the control strain has more biomass than the mutant strain, whether in N-deplete or N-replete media, showing that the mutated enzyme had an effect on growth. A lower biomass productivity in algal strains used for the purpose of lipid accumulation has been previously reported (Hu *et al.*, 2008; Rodolfi *et al*., 2009; Li *et al*., 2010; El-Kassas, 2013). The mutant strain (I58W3) is much less affected by the N deprivation than S1-Wt. This could be explained by the fact that these cells grew more slowly than control cells and subsequently reach the stationary phase later. At 48 h all cultures DW were significantly different than S1-Wt N100. At 96 h only I58W3 N5 has a significant difference in DW. The same trend observed in dry biomass assays can be seen in cell number per mL of culture, where the S1-Wt strain always have more cells than the I58W3 strain (fig 3.2). A decrease in biomass, due to growth inhibition, in fast-growing photosynthetic organisms could be linked to a decrease in chlorophyll levels, alongside other proteins (Kraft *et al.*, 2008; Acquisti *et al.*, 2009; Langner *et al*., 2009; Huo *et al.*, 2011). In fact, I58W3 mutant had a lower chlorophyll *a* and *b* content per mL of culture when compared to S1-Wt strain at 48 and 96h. However when comparing total chlorophyll levels when cell number is equal between strains the same trend is obtained, which indicates that I58W3 cells do not produce as much chlorophyll as S1-Wt, or that the chlorophylls degrade faster. N deprivation seems to affect chlorophyll levels as described previously (Juergens *et al.*, 2015), and consequently presented yellow colour as opposed to green cultures in N replete media.

A B C D

Figure 3.1. Colour differences between S1-Wt and I58W3 *C. reinhardtii* cells grown in standard (A and C) and under nitrogen deprivation (B and D) for 48h.

Table 1. Dry weight (DW) and chlorophyll levels of *C. reinhardtii* cells, wild-type control (Wt-S1) and I58W3 mutant strain grown in Tris-acetate phosphate (TAP) under nitrogen-replete (100% N) or nitrogen-depleted (5%N) conditions, at 48 and 96 hours. Values correspond to average of n = 3 samples. Values correspond to average ± standard error, n=3; asterisks indicate significant differences ($p \leq 0.05$).

	48 H				96 H			
	S1-Wt		I58W3		S1-Wt		I58W3	
	100% N	5% N	100% N	5% N	100% N	5% N	100% N	5% N
DW (mg mL^{-1})	0.56±0.36	0.37±0.14*	0.31±0.15*	0.30±0.23*	0.32±0.08	0.32±0.13	0.39±0.21	0.30±0.08*
Chlorophyll *a* (µg mL^{-1})	4.51±1.36	3.83±1.54	3.01±1.33	2.58±0.73	5.13±0.79	1.66±0.21	3.32±0.50	1.43±0.61
Chlorophyll *b* (µg mL^{-1})	7.46±3.16	7.04±2.83	4.86±2.32	3.96±1.13	10.41±4.64	3.96±1.55	7.70±3.32	2.54±0.48
Total chlorophyll (µg $10^6 cell^{-1}$)	6.53	4.11*	6.91*	4.61*	6.78	1.76*	5.76*	1.99*

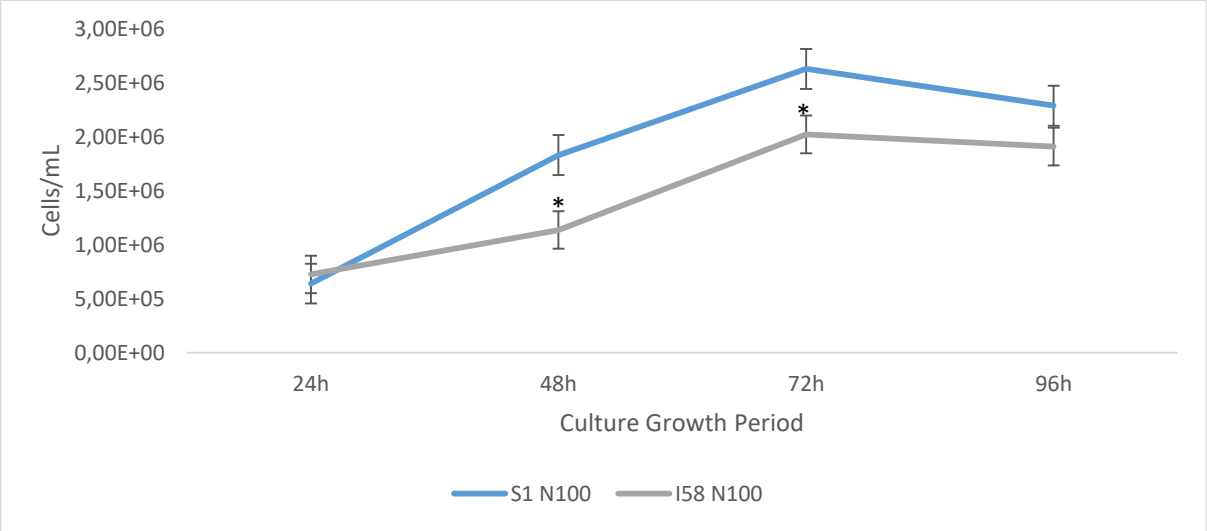

Figure 3.2. Strain number of cells per mL in *C. reinhardtii* S1-Wt control and I58W3 strains measured throughout 5 consecutive days. Values correspond to average ± standard error, n=3; asterisks indicate significant differences ($p \leq 0.05$).

Fig. 3.3 shows culture growth of S1-Wt and I58W3 cells in mixotrophic (under the presence of light and acetate), autotrophic (without acetate but in the presence of light) and heterotrophic (without the presence of light but with acetate) conditions. Mutant I58W3 displayed only a small decrease in growth compared with the wild type under mixotrophic conditions, however it could hardly grow at autotrophic conditions. Under heterotrophic conditions growth of the mutants was indistinguishable from wild-type growth, indicating that the decreased growth of the mutant under autotrophic conditions was caused by a defect in photosynthesis.

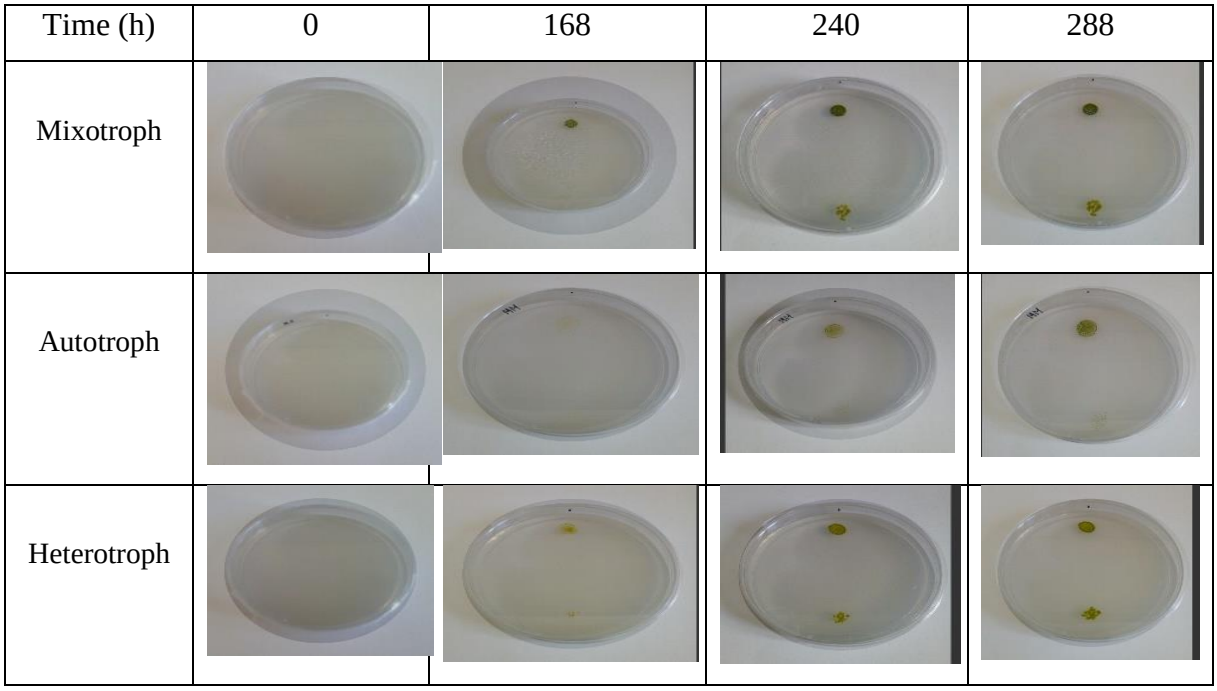

Figure 3.3. Cell growth evolution over time of S1-Wt (upper half of the Petri dish) and I58W3 strains (lower half) under different trophic conditions.

Protein levels seem to be higher in I58W3 than in S1-Wt for the same number of cells at 48 h of growth. At 96 h of N depletion both S1-Wt and I58W3 strains show significantly less protein content (fig. 3.4). A lower amount of proteins under N-depletion has been previously reported in other microalgae such as the diatom *Phaeodactylum tricornutum* (Burcu Ak *et al*., 2015) and in the green alga *Picochlorum sp.* (El-Kassas, 2013). In *C. reinhardtii*, a decrease in protein levels under S deprivation in rubisco mutants has been reported (Pinto *et al*., 2013), and our N deprivation results appear to suggest the same for I58W3 mutants.

Since N is a key element to protein synthesis the decrease in proteins at 96 h was expected, as a prolonged exposure to an N replete media implies a quicker consumption of available N. When this exogenous N is depleted, and in order for protein synthesis to continue, autophagic processes may occur in order to make endogenous N available as a way of *de novo* synthesis so that cells can be able to adapt, such as the *Chlamydomonas* sp. differentiation into sexual gametes which grants it the ability to survive prolonged nutrient stress (Martin and Goodenough, 1975; Wang *et al.*, 2009; Msanne *et al.*, 2012).

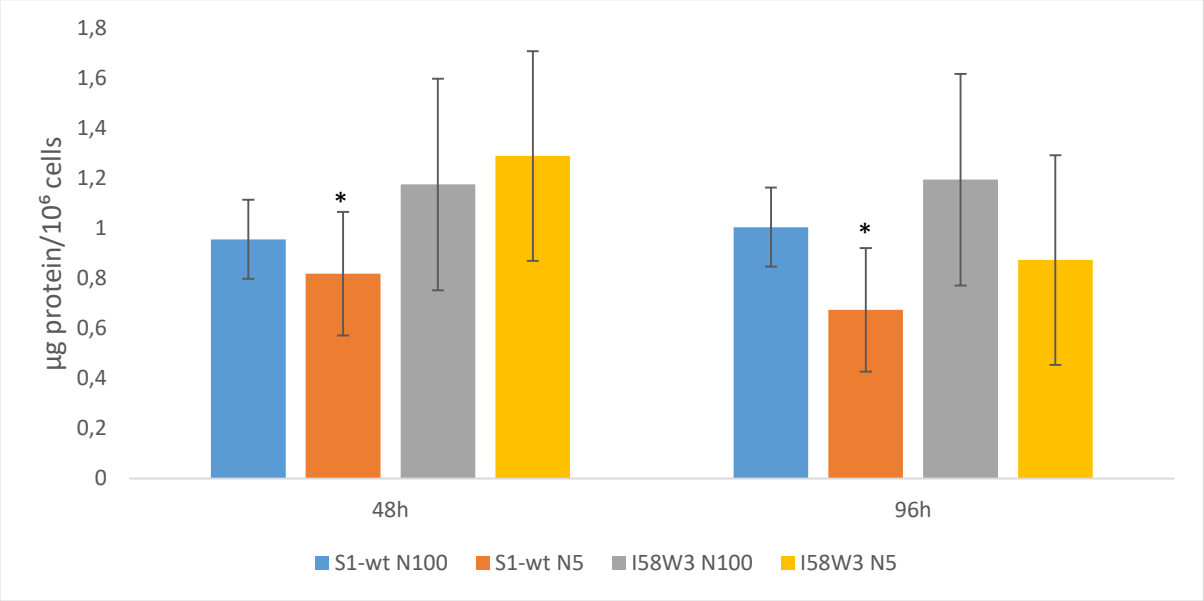

Figure 3.4. Total µg of protein per million cells at 48 and 96h in *C. reinhardtii* wild type (S1-Wt) and I58W3 mutants grown under N-depletion and N-repletion. Values correspond to average ± standard error, n=3; asterisks indicate significant differences ($p \leq 0.05$).

3.2. Rubisco large subunit protein level decreases in I58W3 *C. reinhardtii*

In order to assess and compare Rubisco levels in both strains under stress or in N replete media, western blot analyses were performed. I58W3 strain always presents less amounts of Rubisco large subunit than the control (fig.3.5). It is known that this mutation causes Rubisco to have a lower CO_2 / O_2 specificity possibly due the closure of the central channel (Esquivel *et al.*, 2013).

Rubisco synthesis involves the consumption of N (Evans and Seemann, 1989). It is possible that due to a decrease in N availability these cells cannot compensate the lack of this nutrient and therefore, alongside the mutation, I58W3 shows less Rubisco content than S1-Wt. Previous studies using a different small subunit Rubisco mutant (Y67A) also show a decrease in Rubisco content (Esquível *et al.*, 2006; Esquível *et al.*, 2017).

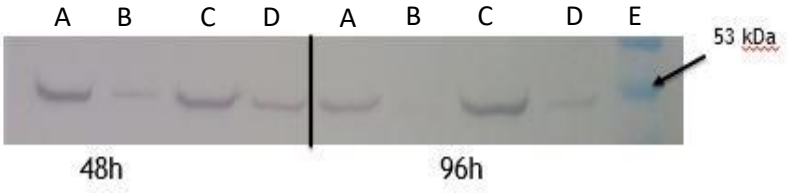

Figure 3.5. Rubisco large subunit band differences between S1-Wt and I58W3 *C. reinhardtii* cells at 48 and 96 hours of culture growth. A – S1-Wt N100; B – I58W3 N100; C – S1-Wt N5; D – I58W3 N5; E – Molecular weight protein ladder. Rubisco large subunit displays a molecular weight of approximately 53 kDa.

Western blot method using an initial specific anti-Rubisco antibody proved to be successful as individual bands with Rubisco large subunit molecular mass (66 kDa) were visible for all samples. Previous work with another Rubisco mutant, Y67A, grown under nutrient stress has also shown a decrease in Rubisco content, which could indicate that I58W3 could have a less stable enzyme structure, such as Y67A (Esquível *et al*., 2006; Pinto *et al*., 2013). These results also seem to indicate that the I58W3 mutation in Rubisco small subunit also seems to affect the large subunit

3.3. Lipid and fatty acid quantifications

Comparison of the storage contents between different growth conditions or different cell lines can be obtained by Red Nile (RN) staining (Alemán-Nava *et al*., 2016). RN binds intracellular neutral lipid droplets (Cooksey *et al.*, 1987; Alemán-Nava *et al*., 2016). By measuring the fluorescence of the dyed sample the value obtained is equivalent to two simultaneous reads, chlorophyll and neutral lipid fluorescence. Using S1-Wt with N-repletion (fig. 3.6) as the baseline for comparison, it is shown that TAG content is lower in S1-Wt N-deprived cells but higher in both N replete medium. It is known that under N deprivation *C. reinhardtii* tend to accumulate TAG (Siaut *et al*., 2011; Msanne *et al*., 2012; Yang *et al*., 2015) which is the case in I58W3 cells, where at 48 and 96 h of the assay seem to have more lipids than control cells. Although the NR test provides an indication of possible differences in storage lipid contents between samples, thin layer and gas chromatography analyses were performed to obtain the exact amount of fatty acids in the cells and the relative contribution of the storage and membrane lipids.

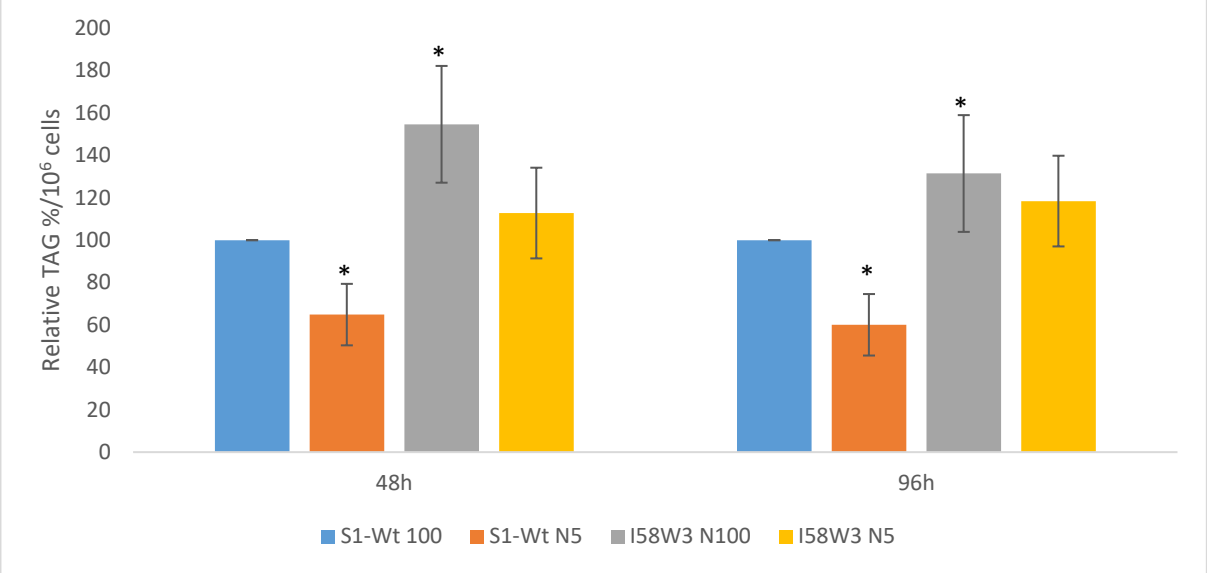

Figure 3.6. Relative TAG levels in *C. reinhardtii* measured by fluorescence intensity of Nile red stained cells minus fluorescence intensity of chlorophyll (before adding the Nile red dye). S1-Wt and I58W3 in normal TAP medium (100% N) and with deficient nitrogen regime (5% N). The S1-Wt 100% N measurements were used as the baseline for comparison with other cells cultures, and results were normalized per 10^6 cells. Values correspond to average ± standard error, n=3; asterisks indicate significant differences ($p \leq 0.05$).

Following lipid extraction and direct methylation, which allows a quick method to assess total lipid content from several samples, gas chromatography was conducted in order to assess fatty acid composition of control and mutant strains (fig. 3.7). Measures taken from samples at 48 h of culture growth show the highest concentrations to be palmitic acid (C16:0), linoleic acid (C18:2) hexadecatrienoic acid (C16:3) and C18:1Δ12 (quantified together due to incomplete separation of the peaks). It has been previously shown that more than 50% of these fatty acids are stored in the TAG, which are a vital element in biodiesel production (Siaut *et al.*, 2011; Shen *et al.*, 2016) Along with C16:3 there are other ω-3 fatty acids which are a part of *C. reinhardtii* composition., such as α-Linolenic acid (C18:3Δ9,12,15), pinolenic acid (C18:3Δ5,9,12) and stearidonic acid (C18:4) which establish this species as an ω-3 source. When comparing both strains the main differences are found on some of these ω-3 fatty acids, mainly C18:3Δ9,12,15 and C18:3Δ5,9,12. Kajikawa *et al.* (2006) have previously reported that ω-13 fatty acid desaturase (FAD) was responsible for the turnover of C18:3Δ9,12,15 into C18:3Δ5,9,12, so a genetic analysis of the gene that expresses that enzyme was performed (3.7 qPCR analysis). Cultures grown under N-repletion show a higher percentage of C16:0 than cells grown under N depletion. Oleic acid (C18:1Δ9) has a higher percentage in N deprived cells, and stearic acid (C18:0) percentages are lower under N stress. N-replete cultures mainly show higher percentages of C16:3 and C18:1Δ12 whereas other fatty acids are evenly present in both stress and normal conditions. Total FA composition *per* g of DW (fig. 3.8) also shows that under N deprivation both strains have a higher FA composition, which indicates that the lack of N can have a role in FA synthesis in *C. reinhardtii*. Fatty acid accumulation under N deprivation has been vastly studied in several species including the diatom *Phaeodactylum tricornutum* (Shen *et al.*, 2016) and in *C. reinhardtii* itself, where it has been found that saturated FAs are present in a higher concentration in cells grown under N deprivation (Sakurai *et al.*, 2014).

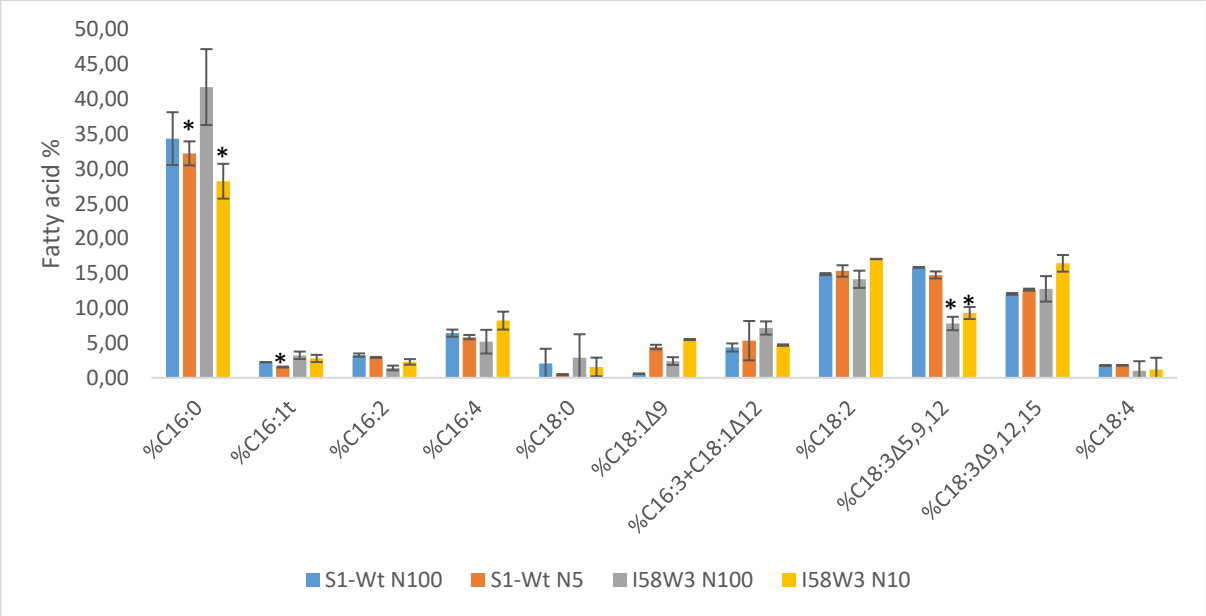

Figure 3.7. Fatty acid composition of S1-Wt and I58W3 in N-replete and N deprived media at 48 h. Values correspond to average ± standard error, n=3; asterisks indicate significant differences ($p \leq 0.05$).

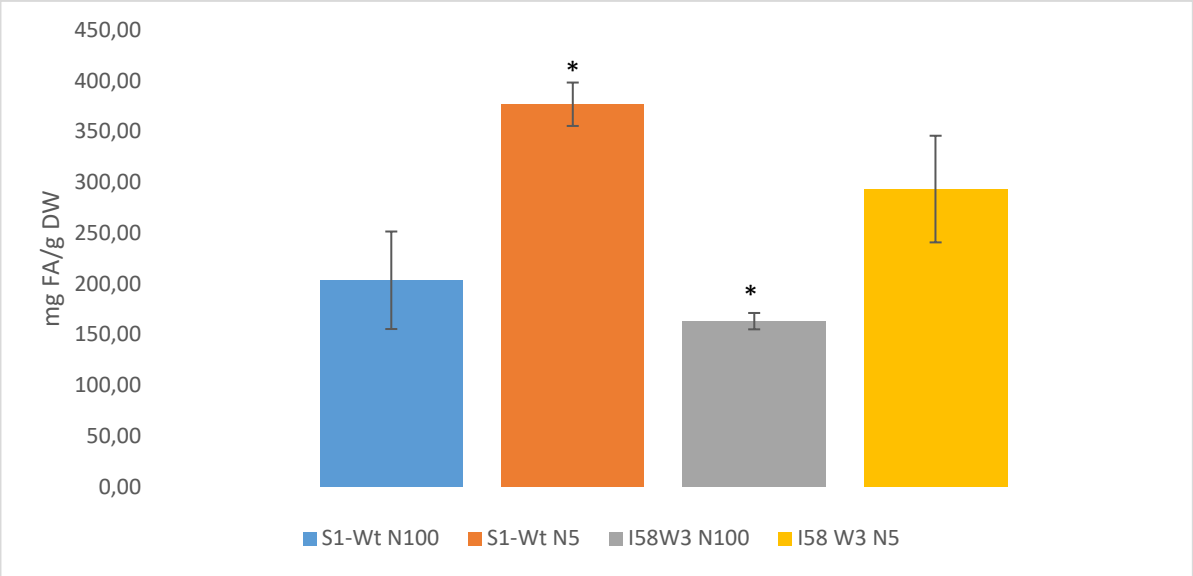

Figure 3.8. Total mg FA/g DW of S1-Wt control and I58W3 *C. reinhardtii* strains under N repletion (N 100%) or depletion (N 5%). Measurements were made at 48h of culture growth. Values correspond to average ± standard error, n=3; asterisks indicate significant differences ($p \leq 0.05$).

TLC allowed the separation of 5 lipid classes, including a mixture of polar lipids (including membrane glycol-and phospholipids) diacylglycerol, free fatty acids, TAG, and an unidentified lipid class X. GC analysis of the fatty acid composition of each class and subsequent class percentage in each strain showed that, although fatty acid composition was not very diverse (data not shown), the TAG percentage was much higher in both the control and mutant strains under N stress, which means that the lack of nitrogen plays a role in TAG accumulation (fig. 3.9). These results are in line with previous conclusions, such as that the major effects of N deprivation in green algae cultures can include an improved biosynthesis and accumulation of lipids, specifically TAG. The amount of lipids in chlorophyta could be raised up to 45% of dry weight by stress induction (Converti *et al.*, 2009). In another study on nitrogen stress responses of different microalgae species, all tested species showed a significant rise in lipid production. The researchers concluded that the increase of lipid concentration in stress exposed refers mainly to neutral lipids, TAG in particular. The observed phenomenon is a result of lipid metabolism shift from membrane lipid synthesis to neutral lipid storage due to environmental stress induction (Hu *et al.*, 2008; El-Kassas, 2013; Esquível *et al.*, 2017). A way to improve TAG biosynthesis has been proposed. By engineering a synthetic pathway that ties N deprivation and starch synthesis it can be possible to increase TAG synthesis, when cells are exposed to N stress, thus prioritising it over starch production (Scaife *et al.*, 2015).

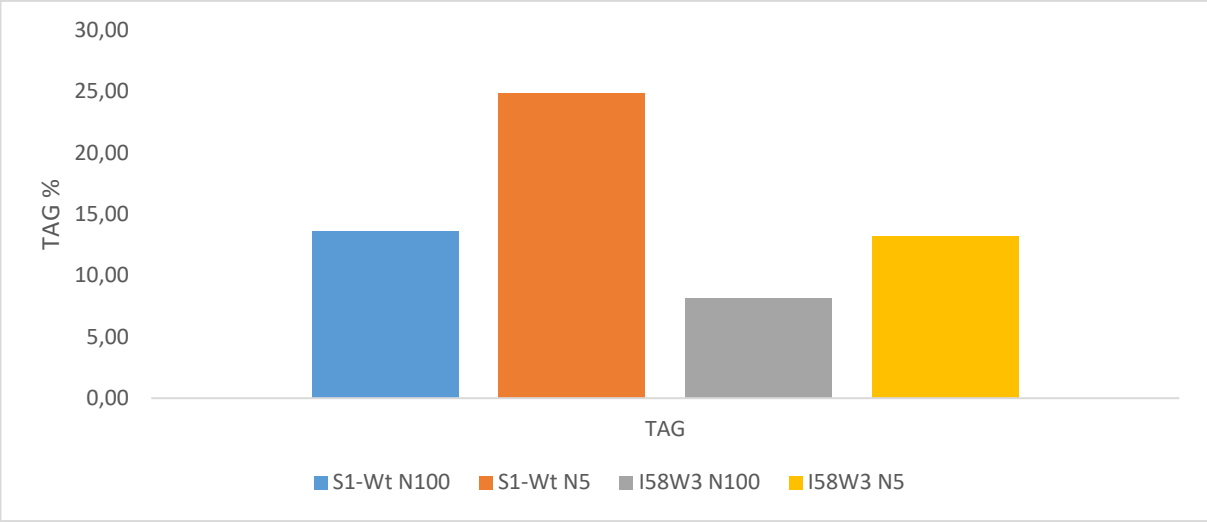

Figure 3.9. TAG percentage in control (S1-Wt) and mutant (I58W3) strains in N-replete (N100) or deplete (N5) media. Measures were made with samples with 48h of cell growth and analysed through thin layer chromatography followed by gas chromatography.

3.4. I58W3 cells have less efficient O_2 production

O_2 electrode measurements carried out at 48 and 96h indicate that I58W3 mutants have a less effective O_2 evolution over time. S1-Wt has a higher ratio of photosynthetic/respiratory activity, which indicates that O_2 production is more effective (fig. 3.10). On the other hand I58W3 spends more O_2 than it produces leading to a less effective overall photosynthetic activity, showing that the mutation induced a slightly higher respiration rate and a significantly lower photosynthetic rate in I58W3 cells than the wild-type. The change in O_2 consumption also makes sense in the N-deprived I58W3 mutant, as a more stressful environment could lead to an

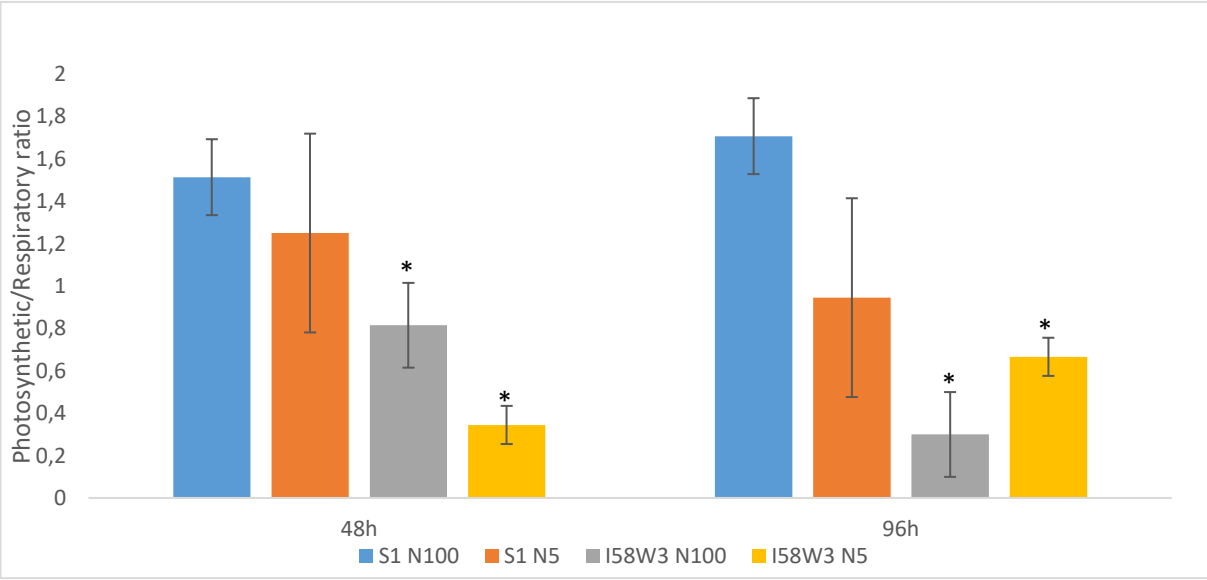

Figure 3.10. Photosynthetic/respiratory ratio at 48h and 96h of *C. reinhardtii* control strain (S1-Wt) and mutant strain (I58W3) in normal TAP medium (100% N) and with deficient nitrogen regime (5% N). Values correspond to average ± standard error, n=3; asterisks indicate significant differences ($p \leq 0.05$).

initial photosynthetic overload, followed by TAG accumulation as another way of maintaining cell functions. Previous reports of a lower CO_2/O_2 specificity in I58W3 cells seem to suggest that in fact the mutation causes a less effective CO_2 fixation in the photosynthetic process (Spreitzer and Salvucci, 2002; Esquivel *et al*., 2013).

3.5. Chlorophyll fluorescence analyses (PAM)

The photosynthetic efficiency of *C. reinhardtii* has been previously reported and shows a significant decrease under N deprivation (Valledor *et al*., 2014; Juergens *et al*., 2015; Esquível *et al.*, 2017). Since chlorophyll fluorescence is highly sensitive to environmental changes, a lack of N results in reduced chlorophyll levels *(*Berges *et al.*, 1996*;* Li *et al.*, 2010; Blaby *et al.*, 2013*;* Juergens *et al.*, 2015).

PAM-derived parameters of OJIP tests are shown in figure 3.11 and in Table 2. Analyses of both strains showed that the photosynthetic processes in I58W3 cells are significantly affected (for $p \leq 0,05$) in all conditions when compared to S1-Wt in N-replete media, except for energy dissipation as heat (DI/CS) where it is higher in N-replete I58W3 cells for both 48 and 96 h. N-deprived control cells also showed lower levels in all conditions ($p \leq 0,05$) except energy transport flux (ET/CS), as it was slightly higher than the N-replete control strain in both time periods.

According to Pinto *et al*. (2013), the low efficiency of PSII could be promoted by a decrease of electron sinks and it has been shown that an inhibition of the Calvin Cycle can lead to an over-reduced state of the photosynthetic electron transport chain, which may result in the generation of reactive oxygen species in PSII that may cause photoinhibition (Skillman, 2008; Antal *et al*., 2011). This is confirmed for the I58W3 strain, as their number of reduction turnovers (N) are much higher than the control strain. These results, alongside the reduced efficiency with which an absorbed photon results in electron transport beyond Q_A- (Φ_{Eo}), seem to explain the reduced electron transport rate in I58W3 cells and could clarify the low photosynthetic efficiency of I58W3 cells. When comparing control and mutant cells, it is clear that PSII is more sensitive under N deprivation. A lower efficiency with which a PSII trapped electron is transferred from Q_A to quinone B ($Q_{B)}$ (Ψ_O) coupled with a lower number of Q_A reducing RCs per PSII antenna chlorophyll (RC/ABS) could explain the problems I58W3 shows in the absorption energy flux as well as in the energy flux trapped by reaction centres being less effective. This could lead to photo oxidation processes that result in thylakoid membrane destruction. The reaction centres are a key component for the primary events in photochemical conversion of light into chemical energy (Allen and Williams, 1998). After light excitation, a charge separation that spans the cell's membrane is formed in the reaction centre. In this case, control strains have a higher concentration of reaction centres than the mutant strain regardless of N deficiency (RC/ABS). This could mean that, overall, mutant strains photosynthetic apparatus is not working as intended, as the conversion of trapped light into energy is affected from the start since they possess a lot less reaction centres, the PSII is gradually inactivated (Melis *et al*., 2000). Even though the rate of photon absorption (ABS/RC) is higher due to a lower level of reaction centres, the trapped energy and electron transport flux (TR_O/RC and ET_O/RC) change

significantly for the N deprived cells but not with the same change as ABS/RC, wich was almost fivefold, at 48h. At 96h the control strain under N deprivation shows a higher level of electron transport flux, which could explain the higher level of ET/CS shown in figure 3.9. Higher energy dissipation levels for I58W3 N replete cells were also reported, and seem to suggest that despite absorbing and utilizing light energy less efficiently than control cells, they also manage

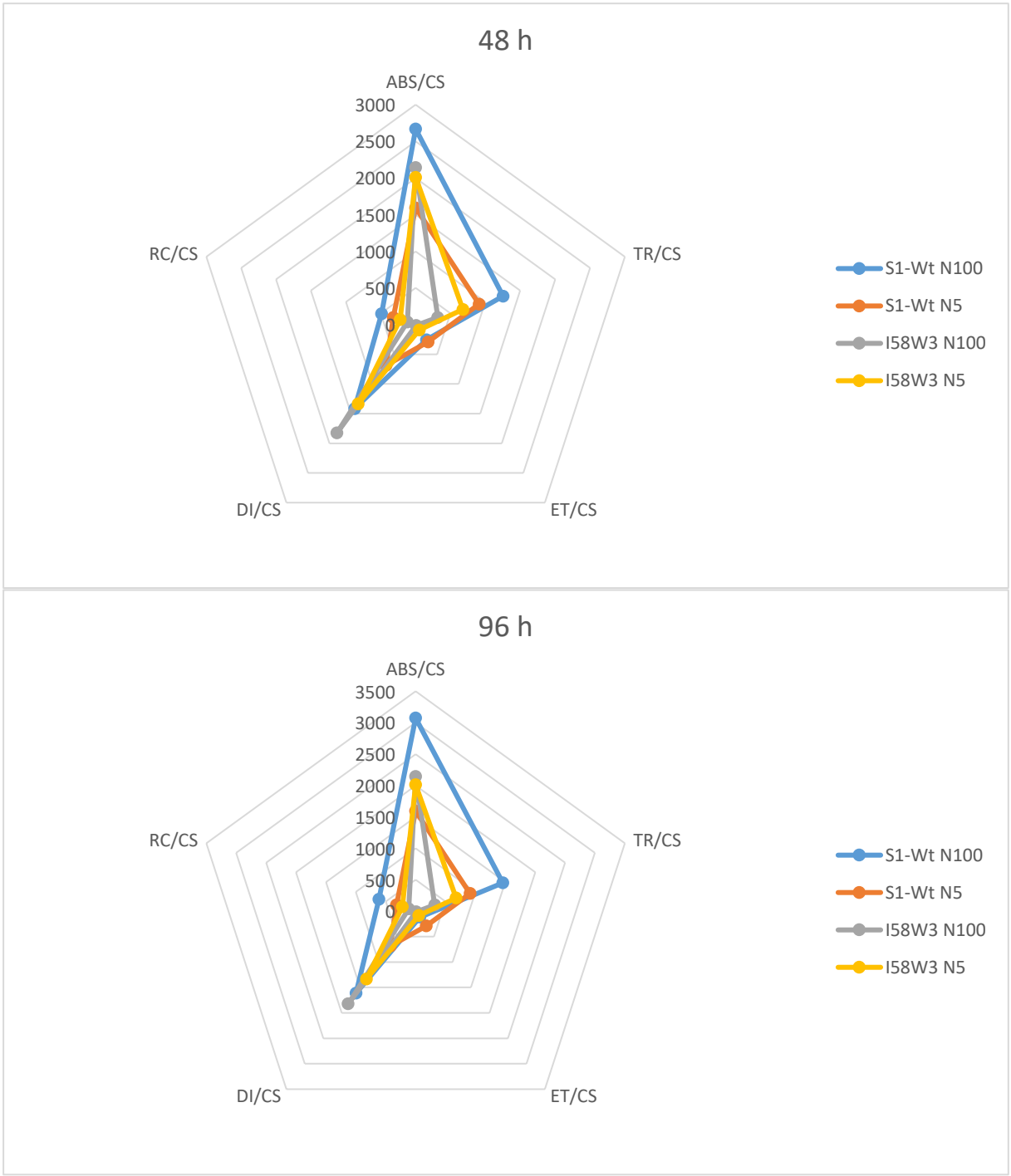

Figure 3.11. Phenomenological energy fluxes in *C. reinhardtii* grown at 48 h (upper graphic) and 96 h (lower graphic) under N-repletion or depletion. Absorbed energy flux per cross-section (ABS/CS); Trapped energy flux per cross-section (TR/CS); Electron transport energy flux per cross-section (ET/CS); dissipated energy flux per cross-section (DI/CS). Reaction Centres per cross section (RC/CS).

to dissipate more through heat, as the quantum yield of energy dissipation as heat (ΦD_O) is higher and the proportion of electron transport to energy dissipation as heat (ET_O/DI_O) is lower in I58W3 cells than in control cells, regardless of N deprivation and at both 48 and 96h.

Table 2. PAM-derived parameters obtained from *C. reinhardtii* grown at 48 h and 96 h under N-repletion or depletion. Number of reduction turnovers (oxidation and re-reduction of Q_A) (N); Efficiency with which an absorbed photon results in electron transport beyond Q_A- (ΦEo); Efficiency or probability with which a PSII trapped electron is transferred from Q_A to Q_B (ΨO); Density or amount or concentration of RCs per absorption energy flux (RC/ABS); Absorbed energy flux per reaction centre (ABS/RC); Trapped energy flux per reaction centre (TRo/RC); Electron transport flux per RC (ETo/RC); Quantum yield of energy dissipation as heat (ΦDo); Proportion of electron transport to energy dissipation as heat (Et_O/Di_O). Values correspond to average, n=3; asterisks indicate significant differences ($p \leq 0.05$).

	48 H					96 H			
	S1-Wt		I58W3			S1-Wt		I58W3	
	100% N	5% N	100% N	5% N		100% N	5% N	100% N	5% N
N	906.16	922.76	3281.68	3162.39		2080.02	1172.18	3282.97	1920.46
ΦEo	0.10	0.18*	0.04*	0.04*		0.04	0.12*	0.04	0.10*
ΨO	0.20	0.32*	0.15	0.13*		0.08	0.23*	0.13	0.31*
RC/ABS	0.91	0.64	0.06*	0.11*		2.61	0.74*	0.05*	0.11*
ABS/RC	5.45	4.96	9.35*	9.07*		5.02	5.77	9.93*	9.38*
TRo/RC	2.56	2.83*	2.72	3.06*		2.39	2.87*	2.65	3.01*
ETo/RC	0.52	0.90*	0.41	0.39*		0.19	0.67*	0.35*	0.94*
ΦDo	0.53	0.43	0.71*	0.66*		0.53	0.50	0.73*	0.68*
Et_O/Di_O	0.18	0.42*	0.06*	0.06*		0.07	0.23*	0.05	0.15

The PAM-derived parameters of RLC of 48 and 96 h old samples without N stress or under N deprivation are shown in Table 3. The mutation tended have a significant impact on ETR_{max}. The α values were lower in I58W3 samples. The photosynthetic efficiency is then lower in the mutant strain, which supports the results obtained with GC analysis. A lower α, especially in the N deprived I58W3, leads to an increase in lipid accumulation due to a metabolic switch from glucose synthesis to lipid storage. Electron transport rate (ETR_{max}) also follows this trend and further supports metabolic photosynthetic abnormalities in I58W3. Photosynthetic rates measured also support this, as lower photosynthetic/respiratory ratios are evident in I58W3. Photoinhibition parameter β was also measured. The same is observed, where I58W3 are more easily inhibited and present significant differences when compared to the control strain. It has been established previously that in *C. reinhardtii* N deprivation can lead to TAG accumulation, but a drawback of that accumulation would be lower photosynthesis rates (Work *et al.*, 2010). Our results with I58W3 follow the same logic.

Table 3. Rapid Light Curve parameters in 48 and 96 h old samples of *C. reinhardtii* under N deprivation and N repletion. Values correspond to average of n = 3 samples. Marked (*) values indicate significant differences between mutant, S1 N5 and S1-Wt N100 control strains ($p \leq 0.05$). α (photosystem II efficiency), ETR_{max} (maximum relative electron transport), β (photoinhibition parameter). Values correspond to average, n=3; asterisks indicate significant differences ($p \leq 0.05$).

	48 h				96 h			
	S1-Wt N100	S1-Wt N5	I58W3 N100	I58W3 N5	S1-Wt N100	S1-Wt N5	I58W3 N100	I58W3 N5
α	0.011	0.006	0*	0*	0.05	0.0027*	0*	0*
ETR_{max}	11.17	11.5	4*	7.333*	5.417*	10.83	4.25*	5.583*
β	0.022	0.020	0.062*	0.057*	0.018	0.013	0.055*	0.053*

3.6. Gene expression analysis by qPCR

Several genes were tested through qPCR (fig. 3.12). Results are shown as fold change of the target gene in the test samples compared to a control sample, after normalization to the expression of the calibrator gene (housekeeping gene, actin) (Livak and Schmittgen, 2001). The mutation causes changes in the photosynthetic apparatus which in turn trigger metabolic changes already described throughout this investigation. In this test we tried to analyse the expression of genes that were considered relevant, taking into account the biochemical and physiological changes observed between control and mutant cells in both growth conditions.

It has been previously reported that, alongside TAG accumulation under N deprivation, there are other changes in *C. reinhardtii* metabolism triggered by both Rubisco mutation and N deprivation. Previous studies with *C. reinhardtii* Rubisco small subunit mutants by Esquível *et al*. (2013; 2017) seem to suggest that the organism's metabolism is affected, reporting low photosynthetic capacity and low effective quantum yield of PSII and decreases in carboxylation rates and CO_2 / O_2 specificity. *SSU* expression appears to be affected the most in the I58W3 mutant under N deprivation, but no significant differences were found. It is known that Rubisco small subunit synthesis is negatively affected by drought (Parry *et al.,* 2002). Regarding TAG accumulation we targeted *DGAT1*, a gene that expresses an acyltransferase which catalyses the conversion of diacylglycerol into TAG. Boyle *et al.* (2012) have reported that *DGAT1* was up-regulated under N deprivation and that it could be a key regulator regarding nitrogen deprivation responses. Our qPCR analysis of this gene also showed a higher *DGAT1* expression under N deprivation. Without N deprivation the I58W3 mutant also showed higher expression concerning the control strain. Regarding FA synthesis, we considered the works of Kajikawa *et al*. (2006), where a fatty acid desaturase (FAD), *CrDES*, is described as having desaturase activity specifically in C18 FA, which is in contrast with previous results from other front-end desaturases. In this case, pinolenic acid is synthesized from linoleic acid. FAD are responsible for the formation of carbon double bonds by removing hydrogen atoms from a fatty acid. Transgenic tobacco plants which constitutively expressed *CrDES* showed higher levels of pinolenic acid with no apparent morphological phenotypes (Kajikawa *et al*,. 2006). No further

studies were conducted regarding how *CrDES* levels could be affected by N deprivation or by a Rubisco mutation. Here we show an impact in the gene expression of *CrDES* under these conditions. In I58W3 the *CrDES* gene was down-regulated in both N deprivation and repletion, which implies a lower FAD activity when compared to the control strain. Sato *et al*. (1997) described a ω-6 FAD, *CrFAD6*, which is an enzyme that catalyses the desaturation of mono to dienoic acids in *C. reinhardtii* chloroplast, specifically oleic (C18:1Δ9) into linoleic acid. Their works with a *CrFAD6* mutant, *hf*-9, concluded that *C. reinhardtii* strains with a lower *CrFAD6* expression have also lower linoleic acid concentrations. Here we found that both N deprivation and the Rubisco mutation have an apparent impact on the FAD6 gene expression of *CRFAD6*. The I58W3 strain again has lower expression levels of FAD6, indicating lower FAD activity and lower conversion of oleic into linolenic acid. The control strain also has a drop in *CrFAD6* expression under N deprivation, indicating that N environmental stress is a key element in both control and I58W3 *CrFAD6* synthesis and subsequent activity. Li *et al* (2012) gave us an insight on a galactolipid lipase (*PGD1*) expression and its impact on TAG production. One of the mutants used in this investigation did not accumulate TAG under N deprivation, which was then attributed to lower expressions of the PDGD1 enzyme. The recombinant enzyme, while expressed in *E. coli*, also hydrolysed monogalactosyldiacylglycerol (MGDG) to produce lyso-MGDG and free FA (X. Li *et al.*, 2012; Li-Beisson *et al*., 2015), which indicates that *C. reinhardtii* synthesizes TAG under N deprivation in two different ways, by *de novo* synthesis and from acyl chains that are already present in membrane lipids. Our results indicate that *PGD1* expression only changed under N deprivation for the control strain, as the mutant strain showed no differences in gene expression. Since this enzyme and its levels are related to TAG accumulation, we believe the results obtained are in accordance with current knowledge. We have shown TAG accumulates in both control and I58W3 strains under N deprivation. Normal or higher levels of *PGD1* expression, which is what we observe, indicate exactly TAG accumulation. It has been previously reported that H_2 production can be caused by nutrient deficiency, such as N or S deprivation (Ghirardi *et al*., 2007; Hemschemeier et al. 2008), through hydrogenase induction. It is believed that hydrogenase activity and synthesis are both tied to O_2 production rates during photosynthesis, which is known to be an inhibitor of H gas production (Forestier *et al*., 2003; Batyrova and Hallenbeck, 2017). With a lower O_2 concentration then it is possible for H_2 production to be more effective. Our results show that hydrogenase activity in I58W3 do not change, indicating no increase in H_2 production. Control strain under N deprivation did show an increase in hydrogenase expression, although H_2 levels were not measured. Culture growth was also undertaken in aerobic conditions, which could prevent H_2 production due to the presence of free O_2. Nutrient deprivation can lead to a gradual inactivation of PSII (Melis *et al*., 2000; Philipps *et al*., 2011; Batyrova *et al*., 2012) and therefore create favourable environments for *C. reinhardtii* cells to produce H_2. Electron transport through cytb_6f facilitates proton pumping from the stroma into the lumen, thus maintaining a proton gradient necessary for ATP production through ATPsyntase (Liran *et al*., 2016). If, under N deprivation, photosynthetic activity seems to be hindered, we targeted and studied how cytb_6f expression would vary under this type of stress. I58W3 analysis reported an increase in cytb_6f expression, which goes against findings reported previously (Valledor *et al*.,

2014), where a fivefold decrease in cytb$_6$f expression under N deprivation was shown. cytb$_6$f complex (E.C. 1.10.99.1) is involved in the electron transport chain from PSII to PSI during photosynthesis, and its gene expression could be tied to the electron transfer efficiency between photosystems. PAM analyses showed that mutant cells have a higher absorbed photon flux per reaction centre, and qPCR results show that the transcripts of this gene are more abundant in both N deprived and replete cells and in N deprived control cells, which could mean there is an attempt at normalizing electron transport.

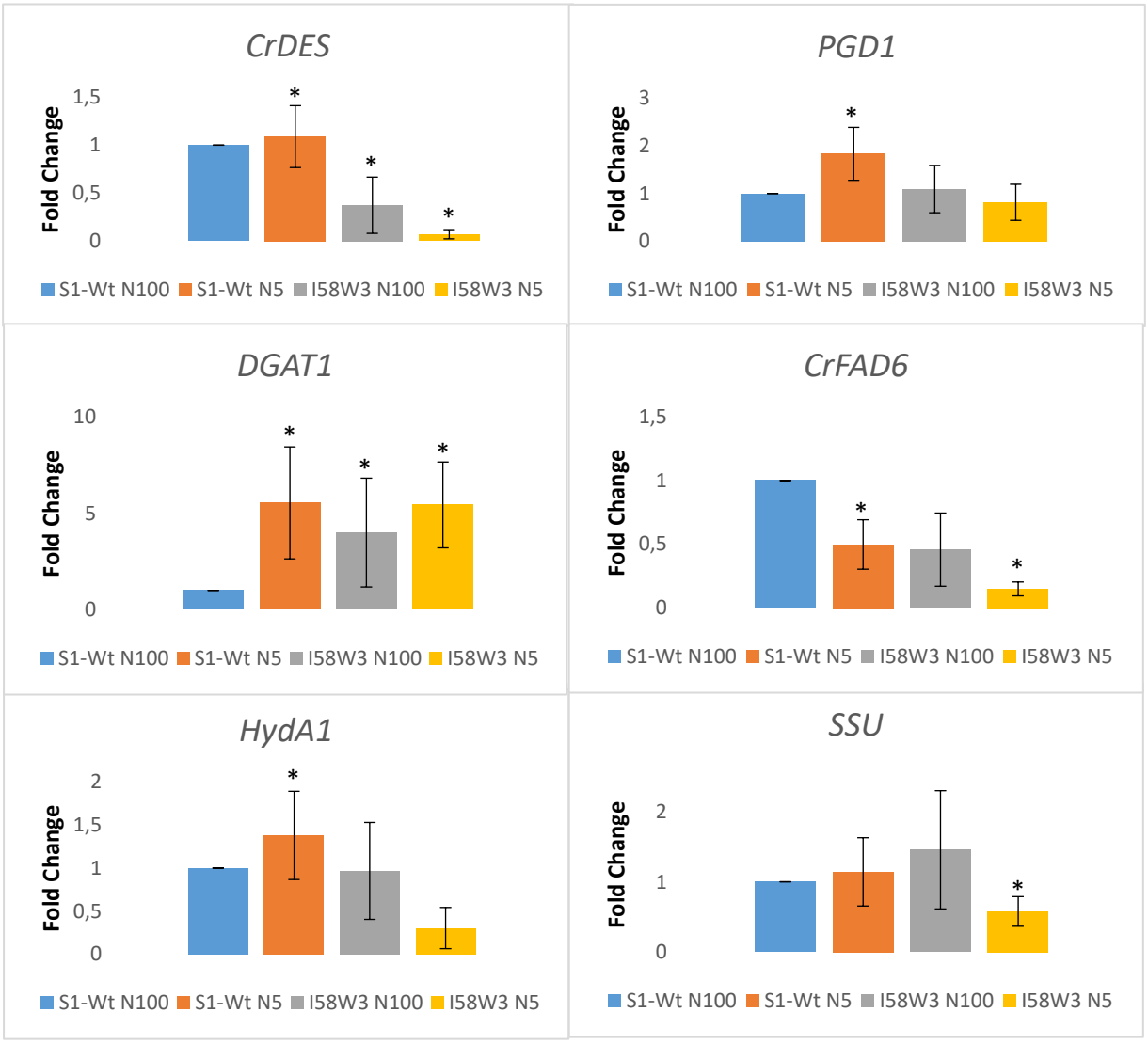

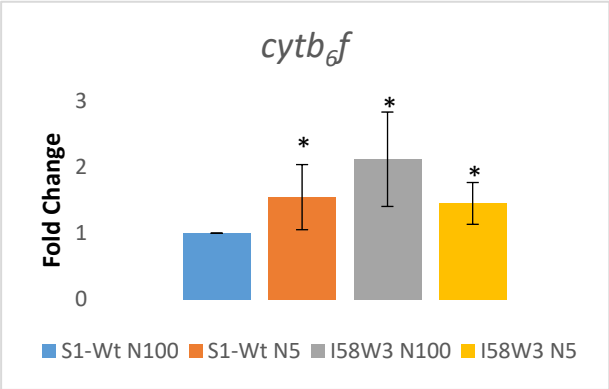

Figure 3.12. Fold change in gene expression calculated using Livak method. Actin was used as the control housekeeping gene. Values correspond to average ± standard error, n=3; asterisks indicate significant differences ($p \leq 0.05$). Fatty acid desaturase (*CrDES* and *CrFAD6*), galactolipase (*PGD1*), diacylglycerol acyltransferase (*DGAT1*), hydrogenase (*HydA1*), Rubisco small subunit (*SSU*) and cytb$_6$f protein.

4. Conclusions and perspectives

Our results show that TAG production from *C. reinhardtii* mutant is a real possibility and culture growth under N deprivation seems to trigger steps that are required in order to increase potential lipid yields, such as a hindered photosynthesis, less O_2 production and TAG accumulation. The energy and carbon required for *de novo* synthesis of TAG could have been redirected from photosynthesis as well as from the external carbon substrates such as acetate present in the culture media (Johnson and Alric 2013; Esquível *et al*., 2017). Overall it seems I58W3 mutant is a capable candidate for biofuel production, although it seems that N deprivation does not impact lipid production as much as desired. N deprived control cells seem to also be an interesting target for lipid accumulation.

PAM results show that the mutant strain has its photosynthetic processes hindered, and that it dissipates more energy than control cells even though it absorbs less. The overall analyses seem to point out that, despite N deprivation, these differences in photosynthetic efficiency are due the mutation, since both strains, under N deprivation and repletion, have a less efficient photosynthesis.

Genetic analyses show that the expression of the genes varies under N deprivation. *DGAT1* is up-regulated, as well as cytb$_6$f. *CrDES* is down-regulated in the mutant strain, which ties in with the GC results that show a lower *CrDES* activity due a higher concentration of linoleic acid. The analysis of more genes related to photosynthesis could complement our results. One possible target is the PsbO protein expressed by the psbo gene, which could be a good indicator of photosynthetic activity as it is a key component of PSII (De Las Rivas and Barber, 2004).

5. References

Acquisti, C., Kumar, S., Elser, J.J. 2009. “Signatures of Nitrogen Limitation in the Elemental Composition of the Proteins Involved in the Metabolic Apparatus.” *Proceedings of the Royal Society B: Biological Sciences* 276(1667): 2605–10. DOI: 10.1098/rspb.2008.1960

Ak, B., Işık, O., Uslu, L., Azgın, C. 2015. “The Effect of Stress Due to Nitrogen Limitation on Lipid Content of *Phaeodactylum tricornutum* (Bohlin) Cultured Outdoor in Photobioreactor.” *Turkish Journal of Fisheries and Aquatic Sciences* 15: 647–52. DOI: 10.4194/1303-2712-v15_3_09

Alemán-Nava, G.S., Cuellar-Bermudez, S.P., Cuaresma, M., Bosma, R., Muylaert, K., Ritmann, B.E., Parra, R. 2016. “How to Use Nile Red , a Selective Fluorescent Stain for Microalgal Neutral Lipids.” *Journal of Microbiological Methods* 128: 74–79. DOI: 10.1016/j.mimet.2016.07.011

Allen, J.P., Williams, J.C. 1998. “Photosynthetic Reaction Centers.” *FEBS Letters* 438(1–2): 5–9. DOI: 10.1016/S0014-5793(98)01245-9

Antal, T.K., Krendeleva, T.E., Rubin, A.B. 2011. “Acclimation of Green Algae to Sulfur Deficiency: Underlying Mechanisms and Application for Hydrogen Production.” *Applied Microbiology and Biotechnology* 89(1): 3–15. DOI: 10.1007/s00253-010-2879-6

Batyrova, K., Tsygankov, A., Kosourov, S.N.. 2012. “Sustained Hydrogen Photoproduction by Phosphorus-Deprived *Chlamydomonas reinhardtii* Cultures.” *International Journal of Hydrogen Energy* 37(10): 8834–39. DOI: 10.1016/j.ijhydene.2012.01.068

Batyrova, K., Hallenbeck, P.C. 2017. “Hydrogen Production by a *Chlamydomonas reinhardtii* Strain with Inducible Expression of Photosystem II.” *International Journal of Molecular Sciences* 18(3). DOI: 10.3390/ijms18030647

Baker, N.R. 2008. “Chlorophyll Fluorescence: A Probe of Photosynthesis in Vivo.” *Annual review of plant biology* 59: 89–113. DOI: 10.1146/annurev.arplant.59.032607.092759

Bensadoun, A., Weinstein, D. 1976. “Assay of Proteins in the Presence of Interfering Materials.” *Analytical Biochemistry* 70(1): 241–50. DOI: 10.1016/S0003-2697(76)80064-4

Berges, J. A., Charlebois, D.O., Mauzerall, D.C., Falkowski, P.G.. 1996. “Differential Effects of Nitrogen Limitation on Photosynthetic Efficiency of Photosystems I and II in Microalgae.” *Plant physiology* 110(2): 689–96. DOI: 10.1104/pp.110.2.689

Bhuyan, A.K. 2010. “On the Mechanism of SDS-Induced Protein Denaturation.” *Biopolymers* 93(2): 186–99. DOI: 10.1002/bip.21318

Blaby, I. K., Glaesener, A.G., Mettler, T., Fitz-Gibbon, S.T., Gallaher, S.D., Liu, B., Boyle, N.R., Kropat, J., Stitt, M., Johnson, S., Benning, C., Pellegrini, M., Casero, D., Merchant, S.S. 2013. “Systems-Level Analysis of Nitrogen Starvation-Induced Modifications of Carbon Metabolism in a *Chlamydomonas reinhardtii* Starchless Mutant.” *The Plant Cell* 25(11): 4305–23. DOI: 10.1105/tpc.113.117580

Bligh, E., Dyer, W. 1959. “A Rapid Method Of Total Lipid Extraction And Purification.” *Canadian Journal of Biochemistry and Physiology* 37.

Borowitzka, M.A., Borowitzka, L.J. 1990. “Micro-algal Biotechnology” *Cambridge University press, Cambridge*

Boyle, N.R., Page, M.D., Liu, B., Blaby, I.K., Casero, D., Kropat, J., Cokus, S.J., Hong-Hermesdorf, A., Shaw, J., Karpowicz, S.J., Gallaher, S.D., Johnson, S., Benning, C., Pellegrini, M., Grossman, A., Merchant, S.S. 2012. “Three Acyltransferases and Nitrogen-Responsive Regulator Are Implicated in Nitrogen Starvation-Induced Triacylglycerol Accumulation in *Chlamydomonas*.” *Journal of Biological Chemistry* 287(19): 15811–25. DOI: 10.1074/jbc.M111.334052

Chen, J.E., Smith, A.G. 2012. “A Look at Diacylglycerol Acyltransferases (DGATs) in Algae.” *Journal of Biotechnology* 162(1): 28–39. DOI: 10.1016/j.jbiotec.2012.05.009

Chernev, P., Goltsev, V., Zaharieva, I., Strasser, R. 2006. “A Highly Restricted Model Approach Quantifying Structural and Functional Parameters of Photosystem II Probed by the Chlorophyll *a* Fluorescence Rise.” *Ecological Engineering and Environment protection* (2): 19–29.

Converti, A., Casazza, A.A., Ortiz, E., Perego, P., Del Borghi, M. “Effect of Temperature and Nitrogen Concentration on the Growth and Lipid Content of *Nannochloropsis oculata* and *Chlorella vulgaris* for Biodiesel Production.” *Chemical Engineering and Processing: Process Intensification* 48(6): 1146–51. DOI: 10.1016/j.cep.2009.03.006

Cooksey, K.E., Guckert, J.B., Williams, S.A., Callis, P.R. 1987. “Fluorometric Determination of the Neutral Lipid Content of Microalgal Cells Using Nile Red.” *Journal of Microbiological Methods* 6(6): 333–45. DOI: 10.1016/0167-7012(87)90019-4

De Las Rivas, J., Barber, J. 2004. “Analysis of the Structure of the PsbO Protein and Its Implications.” *Photosynthesis Research* 81(3): 329–43. DOI: 10.1023/B:PRES.0000036889.44048.e4

Dent, R.M., Han, M., Niyogi, K.K. 2001. “Functional Genomics of Plant Photosynthesis in the Fast Lane Using *Chlamydomonas reinhardtii*.” *Trends in Plant Science* 6(8): 364–71. DOI: 10.1074/jbc.M111.334052

El-Kassas, H.Y. 2013. “Growth and Fatty Acid Profile of the Marine Microalga Picochlorum Sp. Grown under Nutrient Stress Conditions.” *The Egyptian Journal of Aquatic Research* 39(4): 233–39. DOI: 10.1016/j.ejar.2013.12.007

Ellis, R.J. 1979. “The Most Abundant Protein in the World.” *Trends in Biochemical Sciences* 4(11): 241–44. DOI: 10.1074/jbc.M111.334052

Esquível, M.G., Ferreira, R.B., Teixeira, A.R. 2000. “Protein Degradation in C3 and C4 Plants Subjected to Nutrient Starvation. Particular Reference to Ribulose Bisphosphate Carboxylase/oxygenase and Glycolate Oxidase.” *Plant Science* 153(1): 15–23. DOI: 10.1016/S0168-9452(99)00238-1

EsquIvel, M.G.,Genkov, T., Nogueira, A.S., Salvucci, M.S., Spreitzer, R.J. 2013. “Substitutions at the Opening of the Rubisco Central Solvent Channel Affect Holoenzyme Stability and CO2/O2 Specificity but Not Activation by Rubisco Activase.” *Photosynthesis Research* 118(3): 209–18. DOI: 10.1007/s11120-013-9916-0

Esquível, M.G., Matos, A.R., Silva, J.M. 2017. "Rubisco Mutants of *Chlamydomonas reinhardtii* Display Divergent Photosynthetic Parameters and Lipid Allocation." *Applied Microbiology and Biotechnology* 101(13): 5569–80. DOI: 10.1007/s00253-017-8322-5

Esquível, MG., Pinto, T.S., Marín-Navarro, J., Moreno, J. 2006. "Substitution of Tyrosine Residues at the Aromatic Cluster around the βA-βB Loop of Rubisco Small Subunit Affects the Structural Stability of the Enzyme and the in Vivo Degradation under Stress Conditions." *Biochemistry* 45(18): 5745–53. DOI: 10.1021/bi052588y

Evans, J.R., Seemann, J.R. 1989. "The Allocation of Protein Nitrogen in the Photosynthetic Apparatus: Costs, Consequences, and Control." *Plant Biology*.

Fernandez, E., Galvan, A. 2008. "Nitrate Assimilation in *Chlamydomonas*." *Eukaryotic Cell* 7(4): 555–59. DOI: 10.1128/EC.00431-07

Florencio, FJ., Vega, J.M. 1983. "Utilization of Nitrate, Nitrite and Ammonium by *Chlamydomonas reinhardii* - Photoproduction of Ammonium." *Planta* 158(4): 288–93. DOI: 10.1007/BF00397329

Forestier, M., King, P., Zhang, L., Posewitz, M., Schwarzer, S., Happe, T., Ghirardi, M.L., Seibert, M. 2003. "Expression of Two [Fe]-Hydrogenases in *Chlamydomonas reinhardtii* under Anaerobic Conditions." *Eur. J. Biochem.* 270: 2750–58. DOI: 10.1046/j.1432-1033.2003.03656.x

Gallagher, S., Chakavarti, D. 2008. "Immunoblot Analysis." *Journal of Visualized Experiments* (16): 2008. DOI: 10.3791/759

Gallagher, Sean R. 2012. "One-Dimensional SDS Gel Electrophoresis of Proteins. " *Current Protocols in Protein Science* 10.1.1-10.1.44 DOI: 10.1002/0471140864.ps1001s68

Ghirardi, M.L. Posewitz, M., Maness, P., Dubini, A., Yu, J., Seibert, M. 2007. "Hydrogenases and Hydrogen Photoproduction in Oxygenic Photosynthetic Organisms *." *Annual Review of Plant Biology* 58(1): 71–91. DOI: 10.1146/annurev.arplant.58.032806.103848

Giordano, M., Beardall, J., Raven, J.A.. 2005. "CO_2 Concentrating Mechanisms In Algae: Mechanisms, Environmental Modulation, and Evolution." *Annual Review of Plant Biology* 56(1): 99–131. DOI: 10.1146/annurev.arplant.56.032604.144052

Guschina, I.A., Harwood, J.L. 2006. "Lipids and Lipid Metabolism in Eukaryotic Algae." *Progress in Lipid Research* 45(2): 160–86. DOI: 10.1016/j.plipres.2006.01.001

Hames, B.D. 1990. "Gel Electrophoresis of Proteins: A Practical Approach" 2nd Edition. *Oxford University Press*

Happe, T., Kaminski, A. 2002. "Differential Regulation of the Fe-Hydrogenase during Anaerobic Adaptation in the Green Alga *Chlamydomonas reinhardtii*." *Eur. J. Biochem. 269: 1- Happe T and Naber JD* 214: 475–81.

Harris, E.H. 2001. "*Chlamydomonas* as a Model Organism." *Molecular Biology* 52(1): 363–406. DOI: 10.1146/annurev.arplant.52.1.363

Hasan, R., Zhang, B., Wang, L., Shahbazi, A. 2014. "Bioremediation of Swine Wastewater and Biofuel Potential by Using *Chlorella vulgaris, Chlamydomonas reinhardtii,* and *Chlamydomonas debaryana*." *Journal of Petroleum & Environmental Biotechnology* 5(3): 1–20. DOI: 10.4172/2157-7463.1000175

Hemschemeier, A., Fouchard, S., Cournac, L., Peltier, G., Happe, T. 2008. "Hydrogen Production by *Chlamydomonas reinhardtii*: An Elaborate Interplay of Electron Sources and Sinks." *Planta* 227(2): 397–407.

Hu, Q., Sommerfeld, M., Jarvis, E., Ghirardi, M.L., Posewitz, M., Seibert, M., Darzins, A. 2008. "Microalgal Triacylglycerols as Feedstocks for Biofuel Production: Perspectives and Advances." *Plant Journal* 54(4): 621–39. DOI: 10.1111/j.1365-313X.2008.03492.x

Huo, Y. Cho, K.M., Rivera, J.G.L., Monte, E., Shen, C.R., Yan, Y., Liao, J.C. 2011. "Conversion of Proteins into Biofuels by Engineering Nitrogen Flux." *Nature Biotechnology* 29(4): 346–51. DOI: 10.1038/nbt.1789

Johnson, X., Alric, J. 2013. "Central Carbon Metabolism and Electron Transport in *Chlamydomonas reinhardtii*: Metabolic Constraints for Carbon Partitioning between Oil and Starch." *Eukaryotic Cell* 12(6): 776–93. DOI: 10.1128/EC.00318-12

Juergens, M.T., Deshpande, R.R., Lucker, B., Park, J., Wang, H., Gargouri, M., Holguin, F.O., Disbrow, B., Schaub, T., Skepper, J.N., Kramer, D.M., Gang, D.R., Hicks, L.M., Sachar-Hill, Y. 2015. "The Regulation of Photosynthetic Structure and Function during Nitrogen Deprivation in *Chlamydomonas reinhardtii*." *Plant Physiology* 167(2): 558–73. DOI: 10.1104/pp.114.250530

Jungnick, N., Ma, Y., Mukherjee, B., Cronan, J.C., Speed, D.J., Laborde, S.M., Longstreth, D.J., Moroney, J.V. 2014. "The Carbon Concentrating Mechanism in *Chlamydomonas reinhardtii*: Finding the Missing Pieces." *Photosynthesis Research* 121(2–3): 159–73. DOI: 10.1007/s11120-014-0004-x

Kajikawa, M., Yamato, K., Kohzu, Y., Shoji, S., Matsui, K., Tanaka, Y., Sakai, Y., Fukuzawa, H. 2006. "A Front-End Desaturase from *Chlamydomonas reinhardtii* Produces Pinolenic and Coniferonic Acids by ω13 Desaturation in Methylotrophic Yeast and Tobacco." *Plant and Cell Physiology* 47(1): 64–73. DOI: 10.1093/pcp/pci224

Kalaji, H.M., Bosa, K., Kościelniak, J., Hossain, Z. 2011. "Chlorophyll *a* Fluorescence—A Useful Tool for the Early Detection of Temperature Stress in Spring Barley (*Hordeum vulgare* L.)." *OMICS: A Journal of Integrative Biology* 15(12): 925–34. DOI: 10.1089/omi.2011.0070

Kraft, C., Deplazes, A., Sohrmann, M., Peter, M. 2008. "Mature Ribosomes Are Selectively Degraded upon Starvation by an Autophagy Pathway Requiring the Ubp3p/Bre5p Ubiquitin Protease." *Nature Cell Biology* 10(5): 602–10. DOI: 10.1038/ncb1723

Langner, U., Jakob, T., Stehfest, K., Wilhelm, C. 2009. "An Energy Balance from Absorbed Photons to New Biomass for *Chlamydomonas reinhardtii* and *Chlamydomonas acidophila* under Neutral and Extremely Acidic Growth Conditions." *Plant, Cell and Environment* 32(3): 250–58. DOI: 10.1111/j.1365-3040.2008.01917.x

Li, X., Moellering, E.R., Liu, B., Johnny, C., Fedewa, M., Sears, B.B., Kuo, M., Benning, C. 2012. "A Galactoglycerolipid Lipase Is Required for Triacylglycerol Accumulation and

Survival Following Nitrogen Deprivation in *Chlamydomonas reinhardtii*." *The Plant Cell* 24(11): 4670–86. DOI: 10.1105/tpc.112.105106

Li, Y., Han, D., Hu, G., Sommerfeld, M., Hu, Q 2010. "Inhibition of Starch Synthesis Results in Overproduction of Lipids in *Chlamydomonas reinhardtii*." *Biotechnology and Bioengineering* 107(2): 258–68. DOI: 10.1002/bit.22807

Li-Beisson, Y., Beisson, F., Riekhof, W. 2015. "Metabolism of Acyl-Lipids in *Chlamydomonas reinhardtii*." *Plant Journal* 82(3): 504–22. DOI: 10.1111/tpj.12787

Lichtenthaler, H.K. 1987. "Chlorophylls and Carotenoids: Pigments of Photosynthetic Biomembranes." *Methods in Enzymology* 148(C): 350–82. DOI: 10.1016/0076-6879(87)48036-1

Liran, O., Semyatich, R., Milrad, Y., Eilenberg, H., Weiner, I., Yacoby, I. 2016. "Microoxic Niches within the Thylakoid Stroma of Air-Grown *Chlamydomonas reinhardtii* Protect [FeFe]-Hydrogenase and Support Hydrogen Production under Fully Aerobic Environment." *Plant physiology* 172(1): 264–71. DOI: 10.1104/pp.16.01063

Livak, K.J., Schmittgen, T.D. 2001. "Analysis of Relative Gene Expression Data Using Real-Time Quantitative PCR and the 2−ΔΔCT Method." *Methods* 25(4): 402–8. DOI: 10.1006/meth.2001.1262

Mahmood, T., Yang, P. 2012. "Western Blot: Technique, Theory, and Trouble Shooting." *North American Journal of Medical Sciences* 4(9): 429–34. DOI: 10.4103/1947-2714.100998

Martin, N.C., Goodenough, U.W. 1975. "Gametic Differentiation in *Chlamydomonas reinhardtii*. I: Production of Gametes and Their Fine Structure." *Journal of Cell Biology* (18): 587–605.

Matlock, B. 2012. "Assessment of Nucleic Acid Purity." *Technical Note 52646*: 3. http://www.nanodrop.com/Library/T042-NanoDrop-Spectrophotometers-Nucleic-Acid-Purity-Ratios.pdf.

Maxwell, K., Johnson, G.N. 2000. "Chlorophyll Fluorescence - a Practical Guide." *Journal of Experimental Botany* 51(345): 659–68. DOI: 10.1093/jxb/51.345.659

Melis, A., Zhang. L., Forestier, M., Ghirardi, M.L., Seibert, M. 2000. "Sustained Photobiological Hydrogen Gas Production upon Reversible Inactivation of Oxygen Evolution in the Green Alga *Chlamydomonas reinhardtii*." *Plant Physiology* 122, pp. 127–135. DOI:

Merchant, S.S., Prochnik, S.E., Vallon, O., Harris, E.H., Karpowicz, S.J., Witman, G.B., Terry, A., Salamov, A., *et al.* 2007. "The *Chlamydomonas* Genome Reveals the Evolution of Key Animal and Plant Functions." *Science* 318(5848): 245–50. DOI: 10.1126/science.1143609

Merzlyak, M.N., Chivkunova, O.B., Gorelova, O.A., Reshetnikova, I.V., Solovchenko, A.E., Khozin-Goldberg, I., Cohen, Z. 2007. "Effect of Nitrogen Starvation on Optical Properties, Pigments, and Arachidonic Acid Content of the Unicellular Green Alga *Parietochloris incisa* (Trebouxiophyceae, Chlorophyta)." *Journal of Phycology* 43(4): 833–43. DOI: 10.1111/j.1529-8817.2007.00375.x

Meyer, M, Griffiths, H. 2013. "Origins and Diversity of Eukaryotic CO_2-Concentrating

Mechanisms: Lessons for the Future." *Journal of Experimental Botany* 64(3): 769–86. DOI: 10.1093/jxb/ers390S

Miller, R., Wu, G., Deshpande, R., Vieler, A., Gärtner, K., Li, X., Moellering, E.R., Z+auner, S., Cornish, A.J., Liu, B., Bullard, B., Sears, B.B., Kuo, M., Hegg, E.L., Shachar-Hill, Y., Shiu-S., Benning, C. 2010. "Changes in Transcript Abundance in Chlamydomonas reinhardtii Following Nitrogen Deprivation Predict Diversion of Metabolism." *Plant Physiology* 154(4): 1737–52. DOI: 10.1104/pp.110.165159

Minagawa, J., Tokutsu, R. 2015. "Dynamic Regulation of Photosynthesis in *Chlamydomonas reinhardtii*." *Plant Journal* 82(3): 413–28. DOI: 10.1111/tpj.12805

Msanne, J., Xu, D., Konda, A.R., Casas-Mollano, J.A., Awada, T., Cahoon, E.B., Cerutti, H. 2012. "Metabolic and Gene Expression Changes Triggered by Nitrogen Deprivation in the Photoautotrophically Grown Microalgae *Chlamydomonas reinhardtii* and *Coccomyxa* Sp. C-169." *Phytochemistry* 75: 50–59. DOI: 10.1016/j.phytochem.2011.12.007

Park, J., Wang, H., Gargouri, M., Deshpande, R., Skepper, J.N., Holguin, F.O., Juergens, M., Shacahr-Hill, Y., Hicks, L.M., Gang, D.R. 2015. "The Response of *Chlamydomonas reinhardtii* to Nitrogen Deprivation: A Systems Biology Analysis." *Plant Journal* 81(4): 611–24. DOI: 10.1111/tpj.12747

Parry, M.A.J., Andralojc, P.J., Khan, S., Lea, P.J., Keys, A.J 2002. "Rubisco Activity: Effects of Drought Stress." *Annals of Botany* 89(7): 833–39. DOI: 10.1093/aob/mcf103

Philipps, G., Happe, T., Hemschemeier, A. 2011. "Nitrogen Deprivation Results in Photosynthetic Hydrogen Production in *Chlamydomonas reinhardtii*." *Planta* 235(4): 729–45. DOI: 10.1007/s00425-011-1537-2

Pinto, T. S., Malcata, F.X., Arrabça, J.D., Silva, J.M., Spreitzer, R.J., Esquível, M.G. 2013. "Rubisco Mutants of Chlamydomonas reinhardtii Enhance Photosynthetic Hydrogen Production." *Applied Microbiology and Biotechnology* 97(12): 5635–43. DOI: 10.1007/s00253-013-4920-z

Rodolfi, L., Zittelli, G.C., Bassi, N., Padovani, G., Biondi, N., Bonini, G., Tredici, M.R. 2009. "Microalgae for Oil: Strain Selection, Induction of Lipid Synthesis and Outdoor Mass Cultivation in a Low-Cost Photobioreactor." *Biotechnology and Bioengineering* 102(1): 100–112 DOI: 10.1002/bit.22033.

Roessler, P.G. 1990. "Environmental Control of Glycerolipid Metabolism in Microalgae: Commercial Implications and Future Research Directions." *Journal of Phycology* 26(3): 393–99. DOI: 10.1111/j.0022-3646.1990.00393.x

Rupprecht, J. 2009. "From Systems Biology to Fuel - *Chlamydomonas reinhardtii* as a Model for a Systems Biology Approach to Improve Biohydrogen Production." *Journal of Biotechnology* 142(1): 10–20. DOI: 10.1016/j.jbiotec.2009.02.008

Sakurai, K., Moriyama, T., Sato, N. 2014. "Detailed Identification of Fatty Acid Isomers Sheds Light on the Probable Precursors of Triacylglycerol Accumulation in Photoautotrophically Grown *Chlamydomonas reinhardtii*." *Eukaryotic Cell* 13(2): 256–66. DOI: 10.1128/EC.00280-13

Sato, N., Fujiwara, S., Kawaguchi, A., Tsuzuki, M. 1997. "Cloning of a Gene for Chloroplast

ω6 Desaturase of a Green Alga, *Chlamydomonas reinhardtii*." *Journal of biochemistry* 122(6): 1224–32.

Scaife, M.A. Nguyen G.T.D.T., Rico, J., Lambert, D., Helliwell, K.E., Smith, A.G. 2015. "Establishing *Chlamydomonas reinhardtii* as an Industrial Biotechnology Host." *Plant Journal* 82(3): 532–46. DOI: 10.1111/tpj.12781

Schmollinger, S., Mühlhaus, T., Boyler, N.R., Blaby, I.K., Casero, D., Mettler, T., Moseley, J.L., Kropat, J., Sommer, F., Strenkert, D., Hemme, D., Pellegrini, M-., Grossman, A.R., Stitt, M., Schroda, M., Merchant, S.S. 2014. "Nitrogen-Sparing Mechanisms in *Chlamydomonas* Affect the Transcriptome, the Proteome, and Photosynthetic Metabolism." *The Plant Cell* 26(4): 1410–35. DOI: 10.1105/tpc.113.122523

Shen, P., Wang, H., Pan, Y., Meng, Y., Wu, P., Xue, S. 2016. "Identification of Characteristic Fatty Acids to Quantify Triacylglycerols in Microalgae." *Frontiers in Plant Science* 7 DOI: 10.3389/fpls.2016.00162

Shifrin, N.S., Chisholm, S.W. 1981. "Phytoplankton Lipids: Interspecific Differences and Effects of Nitrate, Silicate and Light-Dark Cycles." *Journal of Phycology* 17(4): 374–84. DOI: 10.1111/j.1529-8817.1981.tb00865.x

Siaut, M., Cuiné, S., Cagnon, C., Fessler, B., Nguyen, M., Carrier, P., Beyly, A., Beisson, F., Triantaphylidès, C., Li-Beisson, Y., Peltier, G. 2011. "Oil Accumulation in the Model Green Alga *Chlamydomonas reinhardtii*: Characterization, Variability between Common Laboratory Strains and Relationship with Starch Reserves." *BMC Biotechnology* 11(1): 7. DOI: 10.1186/1472-6750-11-7

Skillman, J.B. 2008. "Quantum Yield Variation across the Three Pathways of Photosynthesis: Not yet out of the Dark." *Journal of Experimental Botany* 59(7): 1647–61. DOI: 10.1093/jxb/ern029

Spreitzer, R.J, Salvucci, M.E. 2002. "Rubisco: Structure, Regulatory Interactions, and Possibilities for a Better Enzyme." *Annual review of plant biology* 53: 449–75. DOI: 10.1146/annurev.arplant.53.100301.135233

Taiz, L., Zeiger, E. 2014. "Plant Physiology and Development" 6th Edition. *Sinauer Associates*

Taylor, T.C., Backlund, A., Bjorhall, K., Spreitzer, R.J., Andersson, I. 2001. "First Crystal Structure of Rubisco from a Green Alga, *Chlamydomonas reinhardtii*." *Journal of Biological Chemistry* 276(51): 48159–64. DOI: 10.1074/jbc.M107765200

Thompson, G.A. 1996. "Lipids and Membrane Function in Green Algae." *Biochimica et Biophysica Acta - Lipids and Lipid Metabolism* 1302(1): 17–45. DOI: 10.1016/0005-2760(96)00045-8

Tsekova, K., Todorova, D., Ganeva., S. 2010. "Removal of Heavy Metals from Industrial Wastewater by Free and Immobilized Cells of *Aspergillus niger*." *International Biodeterioration & Biodegradation* 64(6): 447–51. DOI: 10.1016/j.ibiod.2010.05.003

Valledor, L., Furuhashi, T., Recuenco-Muñoz, L., Wienkoop, S., Weckwerth, W. 2014. "System-Level Network Analysis of Nitrogen Starvation and Recovery in Chlamydomonas reinhardtii Reveals Potential New Targets for Increased Lipid Accumulation." *Biotechnology for Biofuels* 7(1): 171.

Wagener, H. 1965. “Detection and Documentation of Lipids after Thin-Layer Chromatography.” *Nature* 205.

Walker, D. 1987. “The Use of the Oxygen Electrode and Fluorescence Probes in Simple Measurements of Photosynthesis.” DOI: 10.1007/s13398-014-0173-7.2

Wang, Z.T., Ullrich, N., Joo, S., Waffenschmidt, S., Goodenough, U.W. 2009. “Algal Lipid Bodies: Stress Induction, Purification, and Biochemical Characterization in Wild-Type and Starchless *Chlamydomonas reinhardtii*.” *Eukaryotic Cell* 8(12): 1856–68. DOI: 10.1128/EC.00272-09

Work, V.H., Radakovits, R., Jinkerson, R.E., Meuser, J.E., Elliott, L.G., Vinyard, D.J., Laurens, M.L., Diamukes, G.C., Posewitz, M.C. 2010. “Increased Lipid Accumulation in the *Chlamydomonas reinhardtii* sta7-10 Starchless Isoamylase Mutant and Increased Carbohydrate Synthesis in Complemented Strains.” *Eukaryotic Cell* 9(8): 1251–61. DOI: 10.1128/EC.00075-10

Yang, D., Song, D., Kind, T., Ma, Y., Hoefkens, J., Fiehn, O. 2015. “Lipidomic Analysis of *Chlamydomonas reinhardtii* under Nitrogen and Sulfur Deprivation.” *PLoS ONE* 10(9): 1–16. DOI: 10.1371/journal.pone.0137948

Zeraatkar, A.K., Ahmadzadeh, H., Talebi, A.F., Moheimani, N.R., McHenry, M.P. 2016. “Potential Use of Algae for Heavy Metal Bioremediation, a Critical Review.” *Journal of Environmental Management* 181: 817–31. DOI: 10.1016/j.jenvman.2016.06.059

Zhu, X., Govindjee., Baker, N.R., deSturler, E., Ort, D.R., Long, S.P. 2005. “Chlorophyll *a* Fluorescence Induction Kinetics in Leaves Predicted from a Model Describing Each Discrete Step of Excitation Energy and Electron Transfer Associated with Photosystem II.” *Planta* 223(1): 114–33. DOI: 10.1007/s00425-005-0064-4

6. Supplements

Supplement 1 – *Chlamydomonas reinhardtii* media

1.1 – Liquid media and Beij Stock

Liquid media		
TAP Media (1 L)	Beij Stock (for 1 L solution)	Beij Stock (for 1 L solution, with 5% N)
Tris stock (10 mL) Phosphate stock (10 mL) Acetate stock (10 mL) Beij stock (50 mL) Trace elements (1 mL) H_2O (920 mL)	NH_4Cl (8 g) $CaCl2.2H_2O$ (1 g) $MgSO_4.7H_2O$ (2 g) H_2O to 1 L	NH_4Cl (0,4 g) $CaCl2.2H_2O$ (0,25 g) $MgSO_4.7H_2O$ (0,5 g) KCl (1,8 g) H_2O to 1 L
Solid media: add 15 g of Bacto agar to 1 L of liquid TAP media		

1.2 – Stock solutions

Solutions		
Tris stock (1 L)	Phosphate stock	Acetate stock
Trizma base (242,2 g) HCl (149,0 mL) H2O to 1 L	K_2HPO_4 (14,34 g) KH_2PO_4 (7,26 g) H_2O to 1 L	$NaAcetate.3H_2O$ (7,2 g) H_2O to 200 mL

Supplement 2 – Lichtenthaler equations for chlorophyll quantification when dissolved in 100% methanol (v/v)

Chlorophyll a = 16,72 x Abs 665,2 nm – 9,16 x Abs 652,4 nm

Chlorophyll b = 34,09 x Abs 652,4 nm – 15,28 x Abs 665,2 nm

Total cholorophyll = 1,44 x Abs 665,2 nm + 24,93 x Abs 652,4 nm

Supplement 3 – Summary of fluorometric analysis parameters and their description

JIP-test	
Turnover number of Q_A; Total number of electrons transferred into electron transport chain; Number of reduction turnovers (oxidation and re-reduction of Q_A) in the time between turning on the light and T_M	N
Quantum yield of electron transport flux from Q_A to Q_B of PSII; Efficiency with which an absorbed photon results in electron transport beyond Q_A-; Probability that an absorbed photon will move an electron into electron transport further than Q_A-	Φ_{Eo}
Quantum yield of dissipation; Quantum yield of energy dissipation as heat	Φ_{Do}
Efficiency or probability with which a PSII trapped electron is transferred from Q_A to Q_B; Number of reaction centers open at the J-step (at 2 ms)	Ψ_O
Proportion of electron transport to energy dissipation as heat	ET_O/DI_O
Absorbed energy flux per RC; Absorbed photon flux per RC; Rate of photon absorption	ABS/RC
Trapped energy flux per RC; Maximum trapped exciton flux per PSII; Maximum rate of Q_A reduction	TR_O/RC
Electron transport flux per RC; Electron transport flux from Q_A to Q_B per PSII; Rate of electron transport beyond Q_A-	ET_O/RC
Absorbed energy flux per CS; Absorbed photon flux per CS	ABS/CS
Trapped energy flux per CS; Maximum trapped exciton flux per CS	TR/CS
Electron transport flux per CS; Electron transport flux from Q_A to Q_B per CS	ET/CS
Energy dissipation as heat per CS	DI/CS
Density or amount or concentration of RCs per ABS; Number of Q_A reducing RCs per PSII antenna chlorophyll	RC/ABS
Density or amount or concentration of RCs per CS; Number of RCs per CS	RC/CS
Rapid Light Curves (RLC)	
Maximum ETR obtained from the RLC after which photo-inhibition can be observed	ETR_{max}
Photosynthetic efficiency, obtained from the initial slope of the RLC	α
RLC related respiration, obtained from the final slope; Photo-inhibition parameter	β

Supplement 4 – qPCR primers and materials

Gene	Primer Sequence	Gene ID	Protein Location	Annealing Temperature (º C)
CrFAD6	Fw-TACCTCATCTCTATCAGCCCC Rev-TGTCCTCGATCAGGTTGTTCT	Cre13.g590500.t1.1	Chloroplast	Fw – 64 Rev - 62
CrDES	Fw-TGGCCGCGCAGAAGAAG Rev-AGGAAGGGCGTGATGTAGAA	Cre10.g453600.t1.2	Cell membrane	Fw – 56 Rev - 60
HydA1	Fw- GTCTATTCGCGGCAGCTC Rev-GCTGGACATGACTCAAGGG	Cre03.g199800.t1.1	Chloroplast	Fw – 58 Rev - 60
DGAT1	Fw-TGCAGGCAAATGCAGGGTTTC Rev-ACTCGCACCTCCTGCTGACC	Cre01.g045903.t1.1	Chloroplast	Fw – 64 Rev - 66
PGD1	Fw-AGCCAGCTATTGTCGCACTT Rev-CAAGAAATCCGCTGACATCC	Cre07.g344600.t1.2	Unknown	Fw – 60 Rev - 60
SSU	Fw-CTCCTACCTGCCTCCTCTGAC Rev-CATGGGCAGCTTCCACATGG	Cre02.g120150.t1.2	Chloroplast	Fw – 68 Rev - 64
$cytb_6f$	Fw- TGCTAGAGAGCCGTGATGA Rev- TGCGCCGAGTGGTTGAAGT	Cre11.g467689.t1.1	Chloroplast	Fw – 58 Rev - 60
Actin	Fw- GCTTCCAAATGCCTTCCTG Rev-CAAACCCTATGCCTCCTACTGC	Cre09.g397950.t1.1	Cytoskeleton	Fw – 58 Rev - 68